

High-Performance Liquid Chromatography Electrospray Ionization Tandem Mass Spectrometry for the Detection and Quantitation of Pyrrolizidine Alkaloid-Derived DNA Adducts *in Vitro* and *in Vivo*

Peter P. Fu,^{*,†} Ming W. Chou,[†] Mona Churchwell,[†] Yuping Wang,[†] Yuewei Zhao,[†] Qingsu Xia,[†] Gonçalo Gamboa da Costa,[†] M. Matilde Marques,[‡] Frederick A. Beland,[†] and Daniel R. Doerge[†]

National Center for Toxicological Research, Jefferson, Arkansas 72079, and Centro de Química Estrutural, Complexo I, Instituto Superior Técnico, Universidade Técnica de Lisboa, P-1049-001 Lisboa, Portugal

Received November 2, 2009

Pyrrolizidine alkaloid-containing plants are widespread in the world and are probably the most common poisonous plants affecting livestock, wildlife, and humans. Pyrrolizidine alkaloids require metabolism to exert their genotoxicity and tumorigenicity. We have determined that the metabolism of a series of tumorigenic pyrrolizidine alkaloids *in vitro* or *in vivo* generates a common set of (\pm)-6,7-dihydro-7-hydroxy-1-hydroxymethyl-5*H*-pyrrolizine (DHP)-derived DNA adducts that are responsible for tumor induction. The identification and quantitation of the DHP-derived DNA adducts formed *in vivo* and *in vitro* were accomplished previously by ³²P-postlabeling/HPLC methodology. In this article, we report the development of a sensitive and specific liquid chromatography–electrospray ionization–tandem mass spectrometry (HPLC-ES-MS/MS) method to detect DHP-derived DNA adducts formed *in vitro* and *in vivo*. The method is used to quantify the levels of DHP-2'-deoxyguanosine (dG) and DHP-2'-deoxyadenosine (dA) adducts by multiple reaction monitoring (MRM) analysis in the presence of known quantities of isotopically labeled DHP-dG and DHP-dA internal standards. This HPLC-ES-MS/MS method is accurate and precise. When applied to liver samples from rats treated with the pyrrolizidine alkaloids riddelliine and monocrotaline, the method provided significant new information regarding the mechanism of DNA adduct formation.

Introduction

Pyrrolizidine alkaloids are heterocyclic compounds, most of which are derived from esters of basic alcohols, known as the necine bases. The hydrolyzed products of pyrrolizidine alkaloids are a necine base and a necic acid. The structures and numbering system of the several representative necine bases, platynecine, retronecine, heliotridine, and otonecine that form the basis of a variety of commonly studied pyrrolizidine alkaloids are shown in Figure 1.

Pyrrolizidine alkaloids are phytochemicals that are constitutively produced by plants as secondary metabolites for exerting a defense mechanism against insect herbivores (1–3). As a consequence, pyrrolizidine alkaloids are common constituents of hundreds of plant species of different unrelated botanical families distributed in many geographical regions in the world (1, 4–11). Pyrrolizidine alkaloids are found in more than 12 higher plant families of the Angiosperms, among which three families, *Compositae* (*Asteraceae*), *Boraginaceae*, and *Leguminosae* (*Fabaceae*), contain the most toxic pyrrolizidine alkaloids. It has been reported that about 3% of the world's flowering plants contain toxic pyrrolizidine alkaloids (8, 11, 12). More than 660 pyrrolizidine alkaloids and pyrrolizidine alkaloid *N*-oxides have been identified in over 6,000 plants, and about half of them exhibit hepatotoxic activity (4, 5, 13). Toxic pyrrolizidine alkaloid-containing plants grow in South Africa,

Central Africa, the West Indies, China, Jamaica, Canada, Europe, New Zealand, Australia, and the U.S., rendering it highly possible that pyrrolizidine alkaloid-containing plants are the most common poisonous plants affecting livestock, wildlife, and humans (4, 5, 8, 9, 13–15).

Pyrrolizidine alkaloids are among the first naturally occurring carcinogens identified in plants. In 1954, a pure pyrrolizidine alkaloid, retrorsine, was found to induce liver tumors in experimental animals (16). Subsequently, lasiocarpine and riddelliine were found to induce liver tumors in National Toxicology Program (NTP¹) chronic tumorigenicity bioassays (17, 18). Because of the concern about human exposure to genotoxic and tumorigenic pyrrolizidine alkaloids, in 1989, the International Programme on Chemical Safety (IPCS) determined that pyrrolizidine alkaloids are a threat to human health and safety (10). To date, all of the known tumorigenic pyrrolizidine alkaloids are based upon a retronecine, heliotridine, or otonecine structure (5) (Figure 2).

¹ Abbreviations: DHR, dehydroretronecine or (–)-*R*-6,7-dihydro-7-hydroxy-1-hydroxymethyl-5*H*-pyrrolizine; DHP, (\pm)-6,7-dihydro-7-hydroxy-1-hydroxymethyl-5*H*-pyrrolizine; PNK, cloned T4 polynucleotide kinase; MN, micrococcal nuclease; SPD, spleen phosphodiesterase; dG, 2'-deoxyguanosine; dA, 2'-deoxyadenosine; DHP-dG-1 and DHP-dG-2, epimeric pairs of 7-(deoxyguanosin-*N*²-yl)dehydrosupinidine; DHP-dG-3, 9-(deoxyguanosin-*N*²-yl)dehydrosupinidine; DHP-dG-4, 5-(deoxyguanosin-*N*²-yl)dehydrosupinidine; DHP-dA-1 and DHP-dA-2, epimeric pairs of 7-(deoxyadenosin-*N*⁶-yl)dehydrosupinidine; DHP-dA-3, α -(deoxyadenosin-*N*⁶-yl)-dehydrosupinidine; DHP-dA-4, γ -(deoxyadenosin-*N*⁶-yl)dehydrosupinidine; HPLC-ES-MS/MS, high-performance liquid chromatography–electrospray ionization–tandem mass spectrometry; NCTR, National Center for Toxicological Research; NTP, National Toxicology Program; MRM, multiple reaction monitoring; LOD, limit of detection.

* Corresponding author. Tel: +1 870-543-7207. Fax: +1 870-543-7136. E-mail: peter.fu@fda.hhs.gov.

[†] National Center for Toxicological Research.

[‡] Universidade Técnica de Lisboa.

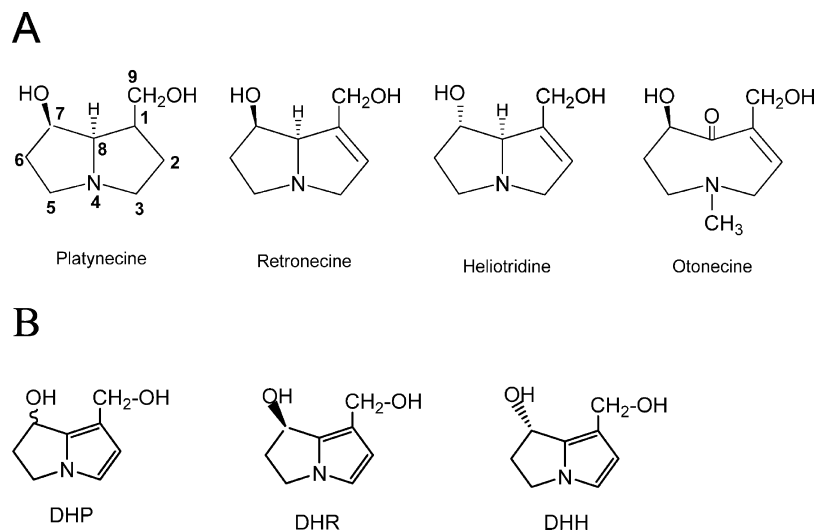
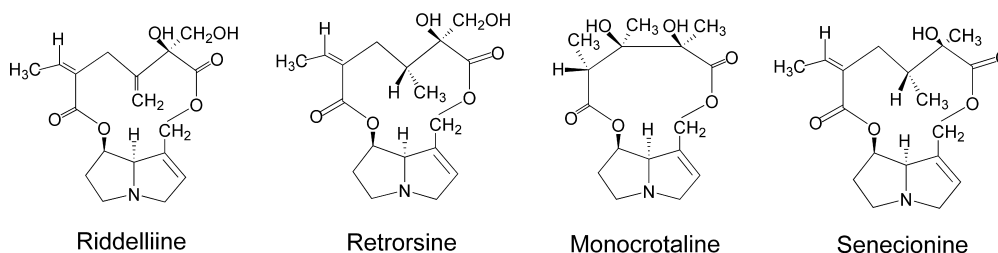
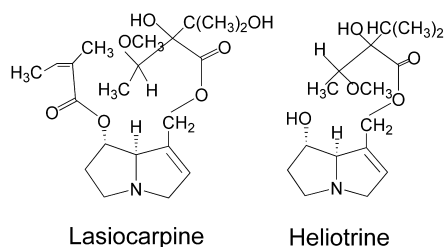


Figure 1. (A) Representative necine bases of pyrrolizidine alkaloids and (B) structures of (\pm)-6,7-dihydro-7-hydroxy-1-hydroxymethyl-5*H*-pyrrolizine (DHP); dehydroretronecine [$(-)$ -(*R*)-6,7-dihydro-7-hydroxy-1-hydroxymethyl-5*H*-pyrrolizine (DHR)]; and dehydroheliotridine [(+)-(*S*)-6,7-dihydro-7-hydroxy-1-hydroxymethyl-5*H*-pyrrolizine (DHH)].

Retronecine-type



Heliotridine-type



Otonecine-type

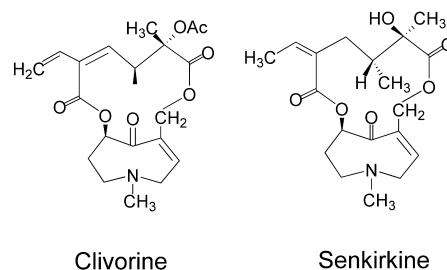


Figure 2. Nomenclature and structures of representative tumorigenic retronecine-, heliotridine-, and otonecine-type pyrrolizidine alkaloids.

Pyrrolizidine alkaloids themselves are not toxic and require metabolic activation to exert their acute and chronic toxicity. The mechanism of tumor formation induced by pyrrolizidine alkaloids was not known until 2001, when it was determined that riddelliine induces liver tumors (i.e., hemangiosarcoma in male and female rats and male mice, and a lower incidence of hepatocellular adenoma and carcinoma in male and female rats) through a genotoxic mechanism mediated by (\pm)-6,7-dihydro-7-hydroxy-1-hydroxymethyl-5*H*-pyrrolizine (DHP)-derived DNA adduct formation (19).

The levels of the DHP-derived DNA adducts correlated closely with the tumorigenic potencies in rats fed different doses of riddelliine (19–21). We subsequently determined that the DHP-derived DNA adduct levels formed *in vivo* in hepatic endothelial cells, the cells of origin for the hemangiosarcomas, were significantly greater than those in parenchymal cells (20). These results indicated that the levels of riddelliine-induced DNA adducts in specific populations of liver cells correlated

with the preferential induction of liver hemangiosarcomas by riddelliine. Furthermore, metabolism of riddelliine by human liver microsomes resulted in a metabolic pattern and DNA adduct profile that were very similar to those formed in rat liver, indicating that the results of *in vivo* and *in vitro* mechanistic studies with experimental rodents are highly relevant to humans (22). Since riddelliine induces liver tumors in rodents and the DHP-derived DNA adducts are responsible for liver tumor induction, these results suggest that riddelliine can be genotoxic to humans via DHP-derived DNA adduct formation. Partly because of these mechanistic findings, the NTP has classified riddelliine as “reasonably anticipated to be a human carcinogen” (23).

Subsequent mechanistic studies on the tumorigenic pyrrolizidine alkaloids, retrorsine, monocrotaline, retronecine, clivorine, lasiocarpine, and heliotrine, conducted under similar experimental conditions, also generated a common set of DHP-derived DNA adducts (24–29). While riddelliine, retrorsine, monocro-

taline, and retronecine are retronecine-type pyrrolizidine alkaloids, clivorine is an otonecine-type, and heliotrine and lasiocarpine are heliotridine-type pyrrolizidine alkaloids (Figure 2). The formation of the same DHP-derived DNA adducts from the metabolism of all of these tumorigenic pyrrolizidine alkaloids indicates that these DHP-derived DNA adducts are potential biomarkers of pyrrolizidine alkaloid exposure and tumorigenicity (5, 25, 30).

Pyrrolizidine alkaloids have long been found as contaminants in many human food sources and may potentially cause worldwide human health problems (1, 5, 6, 13, 31–39). A particular concern is that tumorigenic pyrrolizidine alkaloids have been found in Chinese herbal plants and herbal dietary supplements sold in the U.S. (40), including comfrey, coltsfoot, and borage. We recently reported that the DHP-derived DNA adducts are formed in the livers of female F344 rats gavaged orally with three dietary supplements (comfrey root extract, comfrey compound oil, and coltsfoot root extract) or an extract of a Chinese herbal plant, Flos farfara (Kuan Tong Hua) (40). This indicates that pyrrolizidine alkaloid-containing herbal plants and herbal dietary supplements may pose a human health risk.

DNA adducts are considered to be a biomarker for assessing the risk of chemically induced carcinogenesis. We previously developed a ^{32}P -postlabeling/HPLC method that enabled us to establish that the DHP-derived DNA adducts formed *in vivo* are potential biomarkers of pyrrolizidine alkaloid exposure and tumorigenicity (41). With this method, we identified and quantified the DHP-derived DNA adducts in rodents treated with pure pyrrolizidine alkaloids (e.g., riddelliine, retrorsine, and monocrotaline), Chinese herbal plants, and herbal dietary supplements purchased in the U.S. and Canada. These DNA adducts were also formed from the rat and mouse liver microsomal metabolism of several different pyrrolizidine alkaloids (22, 24–29, 40). We also determined that the same DHP-derived DNA adducts were present in leukocytes of rats fed riddelliine, suggesting that DHP-derived DNA adducts in blood can serve as potential biomarkers of pyrrolizidine alkaloid exposure (30).

There are several limitations associated with ^{32}P -postlabeling/HPLC methods for DNA adduct analysis. These include (i) the risk from exposure to high levels of radioactivity, (ii) DNA adduct instability under the experimental conditions, (iii) frequent problems with enzymatic reactions, and (iv) the lack of structural information. In view of these limitations, it is desirable to develop alternate methods for the detection and quantitation of DHP-derived DNA adducts *in vivo* and *in vitro*, in particular from human samples. In this article, we report the successful development of an HPLC-ES-MS/MS methodology for the identification and quantitation of DHP-derived DNA adducts *in vivo* and *in vitro*.

Experimental Procedures

Caution: Riddelliine, monocrotaline, and DHP are carcinogenic in laboratory animals. They should be handled with extreme care, using proper personal protective equipment and a well-ventilated hood.

Chemicals. Monocrotaline, *o*-bromanil, calf thymus DNA (sodium salt, type I), 2'-deoxyguanosine (dG), 2'-deoxyadenosine (dA), glucose-6-phosphate, glucose-6-phosphate dehydrogenase, and nicotinamide adenine dinucleotide phosphate (NADP⁺) were purchased from the Sigma Chemical Co. (St. Louis, MO). Riddelliine was obtained from the National Toxicology Program (NTP). [$^{15}\text{N}_5$]dG and [$^{15}\text{N}_5$, $^{13}\text{C}_{10}$]dA were obtained from Spectra Stable Isotopes (Columbia, MD). Alkaline phosphatase was acquired from Roche Diagnostics Corporation (Indianapolis, IN). All solvents used were

HPLC grade. (–)-(*R*)-6,7-Dihydro-7-hydroxy-1-hydroxymethyl-5*H*-pyrrolizine (DHR, dehydroretronecine) (Figure 1) was prepared by barium hydroxide-catalyzed hydrolysis of monocrotaline followed by dehydrogenation of the resulting retronecine with *o*-bromanil (19). The 7*R* stereochemistry of DHR was established previously by circular dichroism (CD) spectroscopic analysis (26).

Instrumentation. A Waters HPLC system (Milford, MA), consisting of a Model 600 controller, a Model 996 photodiode array detector, and a 600 pump, was used for the separation and purification of the DHP-derived DNA adducts.

^1H -Nuclear magnetic resonance (NMR) experiments were carried out at 301 K on a Bruker AM 500 spectrometer (Bruker Instruments, Billerica, MA) operating at 500 MHz. Samples were dissolved in DMSO-*d*₆ or DMSO-*d*₆ with a trace of D₂O. NOE difference and homonuclear decoupling experiments were conducted to assist in assigning proton resonances.

Treatment of Rats with Pyrrolizidine Alkaloids. Procedures involving the care and handling of rats were reviewed and approved by the National Center for Toxicological Research (NCTR) Laboratory Animal Care and Use Committee. Female F344 rats were obtained from the NCTR breeding colony as weanlings and maintained on a 12-h light–dark cycle. At 8–10 weeks of age, the rats were orally gavaged for 3 consecutive days with riddelliine, at daily doses of 0, 0.1, 1, 2, and 5 mg/kg body weight in 0.5 mL of 75% DMSO, or with monocrotaline, at daily doses of 1 and 5 mg/kg in the same solvent and volume. Twenty-four hours after the last dose, the rats were sacrificed by exposure to CO₂ followed by exsanguination. Livers were removed, rinsed with cold saline, and stored at –70 °C before DNA was isolated for DNA adduct analysis. DNA samples were extracted using RecoverEase DNA Isolation Kits (Stratagene, Cedar Creek, TX) according to the manufacturer's instructions. The concentration of the DNA was determined spectrophotometrically.

National Toxicology Program (NTP) Female F344 Rat Liver Samples. Riddelliine-modified rat liver DNA was obtained from female F344 rats treated by gavage with riddelliine in a study conducted by the NTP (42). The rats had been treated under the same experimental conditions used for the two year chronic tumorigenicity study, with the exception that there were six animals per dose group and that the animals were sacrificed after six months of treatment. Briefly, female F344/N rats (7–8 weeks old) were gavaged with 0, 0.01, 0.033, 0.1, 0.33, or 1.0 mg of riddelliine/kg body weight in 0.1 M phosphate buffer five times a week and continued until sacrifice at six months after the first dosing day. After sacrifice, liver tissue was collected, stored at –78 °C, and shipped by the NTP to NCTR for DNA adduct analysis. Rat liver DNA was isolated according to the method of Beland et al. (43).

Synthesis of DHP-dG and DHP-dA Adducts. DHP-dG adducts were prepared by an adaptation of the method of Robertson (44). Briefly, to a solution of dG (53 mg, 0.2 mmol) in 10 mL of 25 mM potassium phosphate (pH 7.4) was added DHR (15 mg, 0.1 mmol) under argon over a period of 5 min. The reaction mixture was heated at 37 °C for 15 h. After cooling, the reaction mixture was filtered through a 0.22- μm Millipore filter to remove insoluble materials. The solvent was removed under vacuum, and the resulting residue was separated by HPLC using a Prodigy 5 μm ODS column (Phenomenex, Torrance, CA, 4.6 mm \times 250 mm), by eluting with a methanol and water linear gradient (0–20 min, 20–30% methanol; 30–50 min 30–50% methanol). The flow rate was 1.0 mL/min, and UV absorbance was monitored at 254 nm. DHP-dA adducts were prepared similarly, with the exception that for the HPLC separation, the UV wavelength was set at 266 nm.

The yield of DHP-dA adduct formation is very low. In order to obtain sufficient amounts of pure DHP-dA adducts for structural determination by ^1H NMR spectroscopic analyses and for determination of their UV molar extinction coefficients, 8.0 g of monocrotaline was used to prepare retronecine (2.8 g, 75% yield) (19). Dehydrogenation of the retronecine (2.8 g) with *o*-bromoanil produced DHR (2.14 g, 77% yield) (19), which when reacted with dA (14 g) generated a mixture of four DHP-dA adducts. Upon HPLC purification, pure DHP-dA-1 and DHP-dA-2 were obtained.

On the basis of ^1H NMR spectroscopic analysis in the presence of a known quantity of *tert*-butanol as internal standard, 3.8 mg of DHP-dA-1 (0.07% yield) and 3.6 mg of DHP-dA-2 (0.067% yield) were obtained.

^1H NMR spectroscopic data for each of the isolated adducts follow.

DHP-dG-1. ^1H NMR (DMSO- d_6) δ 2.21–2.25 (1H, m, dG-H2''), 2.34–2.38 (1H, m, DHP-H6b), 2.62–2.68 (1H, m, dG-H2'), 2.86–2.90 (1H, m, DHP-H6a), 3.49–3.54 (1H, m, dG-H5''), 3.57–3.60 (1H, m, dG-H5'), 3.80–3.83 (1H, m, dG-H4'), 3.89–3.94 (1H, m, DHP-H5b), 3.99–4.05 (1H, m, DHP-H5a), 4.28 (1H, bd, DHP-H9b), 4.32 (1H, bd, DHP-H9a), 4.38–4.40 (1H, m, dG-H3'), 4.51 (1H, bs, OH/NH), 4.87 (1H, bt, OH/NH), 5.25–5.28 (2H, m, DHR-H7, OH/NH), 6.09 (1H, d, $J = 2.6$, DHP-H2), 6.20 (1H, dd, $J \sim 7$, dG-H1'), 6.66 (1H, d, $J = 2.6$, DHP-H3), 6.73 (1H, bs, OH/NH), 7.93 (1H, s, dG-H8), 10.31 (1H, s, dG-NH1).

DHP-dG-1. ^1H NMR (DMSO- d_6 /D $_2$ O) δ 2.21–2.26 (1H, m, dG-H2''), 2.31–2.37 (1H, m, DHP-H6b), 2.61–2.67 (1H, m, dG-H2'), 2.83–2.90 (1H, m, DHP-H6a), 3.80–3.83 (1H, m, dG-H4'), 3.87–3.91 (1H, m, DHP-H5b), 3.99–4.03 (1H, m, DHP-H5a), 4.25 (1H, d, $J = 12$, DHP-H9b), 4.29 (1H, d, $J = 12$, DHP-H9a), 4.37–4.39 (1H, m, dG-H3'), 5.25–5.27 (1H, m, DHP-H7), 6.08 (1H, d, $J = 2.5$, DHP-H2), 6.19 (1H, dd, $J \sim 7$, dG-H1'), 6.65 (1H, d, $J = 2.5$, DHP-H3), 7.91 (1H, s, dG-H8).

DHP-dG-2. ^1H NMR (DMSO- d_6) δ 2.21–2.26 (1H, m, dG-H2''), 2.34–2.39 (1H, m, DHP-H6b), 2.62–2.68 (1H, m, dG-H2'), 2.86–2.90 (1H, m, DHP-H6a), 3.49–3.54 (1H, m, dG-H5''), 3.57–3.60 (1H, m, dG-H5'), 3.81–3.83 (1H, m, dG-H4'), 3.89–3.94 (1H, m, DHP-H5b), 4.00–4.05 (1H, m, DHP-H5a), 4.29–4.34 (1H, m, DHP-H9b), 4.32–4.34 (1H, m, DHP-H9a), 4.38–4.40 (1H, m, dG-H3'), 4.51 (1H, t, OH/NH), 4.87 (1H, t, OH/NH), 5.25–5.28 (2H, m, DHP-H7, OH/NH), 6.09 (1H, d, $J = 2.5$, DHP-H2), 6.20 (1H, dd, $J \sim 7.1$, dG-H1'), 6.66 (1H, d, $J = 2.5$, DHP-H3), 6.73 (1H, bs, OH/NH), 7.92 (1H, s, dG-H8), 10.28 (1H, s, dG-NH1).

DHP-dG-2. ^1H NMR (DMSO- d_6 /D $_2$ O) δ 2.21–2.23 (1H, m, dG-H2''), 2.34–2.36 (1H, m, DHP-H6b), 2.63–2.67 (1H, m, dG-H2'), 2.83–2.90 (1H, m, DHP-H6a), 3.80–3.83 (1H, m, dG-H4'), 3.87–3.92 (1H, m, DHP-H5b), 4.00–4.03 (1H, m, DHP-H5a), 4.26 (1H, d, $J = 12$, DHP-H9b), 4.30 (1H, d, $J = 12$, DHP-H9a), 4.36–4.38 (1H, m, dG-H3'), 5.25–5.27 (1H, m, DHP-H7), 6.08 (1H, d, $J = 2.5$, DHP-H2), 6.19 (1H, dd, $J \sim 7$, dG-H1'), 6.65 (1H, d, $J = 2.5$, DHP-H3), 7.91 (1H, s, dG-H8).

DHP-dG-3. ^1H NMR (DMSO- d_6) δ 2.19–2.26 (2H, m, dG-H2'', DHP-H6b), 2.54–2.68 (2H, m, dG-H2', DHP-H6a), 3.48–3.53 (1H, m, dG-H5''), 3.57–3.59 (1H, m, dG-H5'), 3.81–3.85 (2H, m, dG-H4', DHP-H5b), 3.99–4.03 (1H, m, DHP-H5a), 4.23–4.28 (1H, m, DHP-H9b), 4.31–4.37 (1H, m, DHP-H9a), 4.35–4.38 (1H, m, dG-H3'), 4.81 (1H, m, OH/NH), 5.06–5.08 (1H, m, DHP-H7), 5.14–5.15 (1H, m, OH/NH), 5.26–5.27 (1H, m, OH/NH), 6.09 (1H, d, $J = 2.6$, DHP-H2), 6.18 (1H, m, dG-H1'), 6.34 (1H, m, OH/NH), 6.61 (1H, d, $J = 2.5$, DHP-H3), 7.91 (1H, s, dG-H8), 10.40 (1H, s, dG-NH1).

DHP-dG-3. ^1H NMR (DMSO- d_6 /D $_2$ O) δ 2.18–2.25 (2H, m, dG-H2'', DHP-H6b), 2.55–2.66 (2H, m, dG-H2', DHP-H6a), 3.78–3.83 (2H, m, dG-H4', DHP-H5b), 3.98–4.03 (1H, m, DHP-H5a), 4.24 (1H, two sets of d, $J = 14$, DHP-H9b), 4.32 (1H, two sets of d, DHP-H9a), 4.33–4.38 (1H, m, dG-H3'), 5.03–5.08 (1H, m, DHP-H7), 6.07 (1H, d, $J = 2.7$, DHP-H2), 6.19 (1H, m, dG-H1'), 6.60 (1H, d, $J = 2.5$, DHP-H3), 7.89 (1H, s, dG-H8).

DHP-dG-4. ^1H NMR (DMSO- d_6) δ 2.18–2.24 (1H, m, dG-H2''), 2.34–2.37 (1H, m, DHP-H6b), 2.56–2.65 (2H, m, dG-H2', DHP-H6a), 3.49–3.53 (1H, m, dG-H5''), 3.54–3.57 (1H, m, dG-H5'), 3.82 (1H, m, dG-H4'), 3.86–3.92 (1H, m, DHP-H7b), 3.95–4.00 (1H, m, DHP-H7a), 4.25–4.32 (1H, m, DHP-H9b), 4.33–4.36 (1H, m, DHP-H9a), 4.33–4.37 (1H, m, dG-H3'), 4.76 (1H, dd, DHP-H5), 4.85 (1H, bs, OH/NH), 5.25 (1H, d, OH/NH), 6.12 (1H, d, DHP-H2), 6.18 (1H, m, dG-H1'), 6.43 (1H, bs, OH/NH), 6.70 (1H, two sets of d, DHP-H3), 7.90 (1H, s, dG-H8), 8.56 (1H, s, OH/NH), 10.38 (1H, bs, dG-NH1).

DHP-dG-4. ^1H NMR (DMSO- d_6 /D $_2$ O) δ 2.19–2.24 (1H, m, dG-H2''), 2.34–2.39 (1H, m, DHP-H6b), 2.56–2.65 (2H, m, dG-H2',

DHP-H6a), 3.82 (1H, m, dG-H4'), 3.84–3.90 (1H, m, DHP-H7b), 3.92–3.97 (1H, m, DHP-H7a), 4.26 (1H, t, $J = 14$, DHP-H9b), 4.35 (1H, two sets of d, $J = 14.2$, DHP-H9a), 4.35 (1H, m, dG-H3'), 4.74 (1H, dd, $J = 6.4, 7.6$, DHP-H5), 6.11 (1H, d, $J = 2.7$, DHP-H2), 6.17 (1H, m, dG-H1'), 6.68 (1H, two sets of d, $J = 2.7$, DHP-H3), 7.89 (1H, s, dG-H8).

DHP-dA-1. ^1H NMR (DMSO- d_6) δ 2.23–2.31 (1H, m, dA-H2''), 2.35–2.47 (1H, m, DHP-H6b), 2.68–2.78 (1H, m, dA-H2'), 2.85–2.93 (1H, m, DHP-H6a), 3.49–3.56 (1H, two sets of d, $J = 4.5$, dA-H5''), 3.60–3.66 (1H, two sets of d, $J = 4.5$, dA-H5'), 3.85–3.93 (2H, m, DHP-H5b, dA-H4'), 4.01–4.25 (3H, m, DHP-H5a, H9a, H9b), 4.38–4.45 (1H, m, dA-H3'), 4.48 (1H, bs, OH), 5.10–5.45 (2H, bs, overlapped, OH), 5.78 (1H, bs, DHP-H7), 6.04–6.10 (1H, two sets of d, $J = 2.5$, DHP-H2), 6.35–6.38 (1H, dd, dA-H1'), 6.60–6.67 (1H, two sets of d, $J = 2.5$, DHP-H3), 8.07 (1H, bs, dA-N6H), 8.27 (1H, bs, dA-H8), 8.35 (1H, s, dA-H2).

DHP-dA-1. ^1H NMR (DMSO- d_6 /D $_2$ O) δ 2.25–2.31 (1H, m, dA-H2''), 2.33–2.47 (1H, m, DHP-H6b), 2.67–2.73 (1H, m, dA-H2'), 2.87–2.96 (1H, m, DHP-H6a), 3.48–3.56 (1H, two sets of d, $J = 4.5$, dA-H5''), 3.59–3.62 (1H, two sets of d, $J = 4.5$, dA-H5'), 3.84–3.92 (2H, m, DHP-H5b, dA-H4'), 4.04–4.23 (3H, m, DHP-H5a, H9a, H9b), 4.37–4.43 (1H, m, dA-H3'), 5.72 (1H, bs, DHP-H7), 6.04–6.06 (1H, two sets of d, $J = 2.5$, DHP-H2), 6.34 (1H, dd, dA-H1'), 6.59–6.65 (1H, two sets of d, $J = 2.5$, DHP-H3), 8.25 (1H, s, dA-H8), 8.32 (1H, s, dA-H2).

DHP-dA-2. ^1H NMR (DMSO- d_6) δ 2.23–2.32 (1H, m, dA-H2''), 2.34–2.45 (1H, m, DHP-H6b), 2.68–2.78 (1H, m, dA-H2'), 2.84–2.94 (1H, m, DHP-H6a), 3.47–3.56 (1H, m, dA-H5''), 3.57–3.66 (1H, m, dA-H5'), 3.81–3.94 (2H, m, DHP-H5b, dA-H4'), 4.04–4.25 (3H, m, DHP-H5a, H9a, H9b), 4.41 (1H, bs, dA-H3'), 4.47 (1H, bs, OH), 5.25 (1H, bs, OH), 5.33 (1H, bs, OH), 5.78 (1H, bs, DHP-H7), 6.06 (1H, d, $J = 2.0$, DHP-H2), 6.35–6.38 (1H, dd, dA-H1'), 6.60–6.67 (1H, two sets of d, $J = 2.0$, DHP-H3), 8.06 (1H, bs, dA-N6H), 8.27 (1H, bs, dA-H8), 8.35 (1H, s, dA-H2).

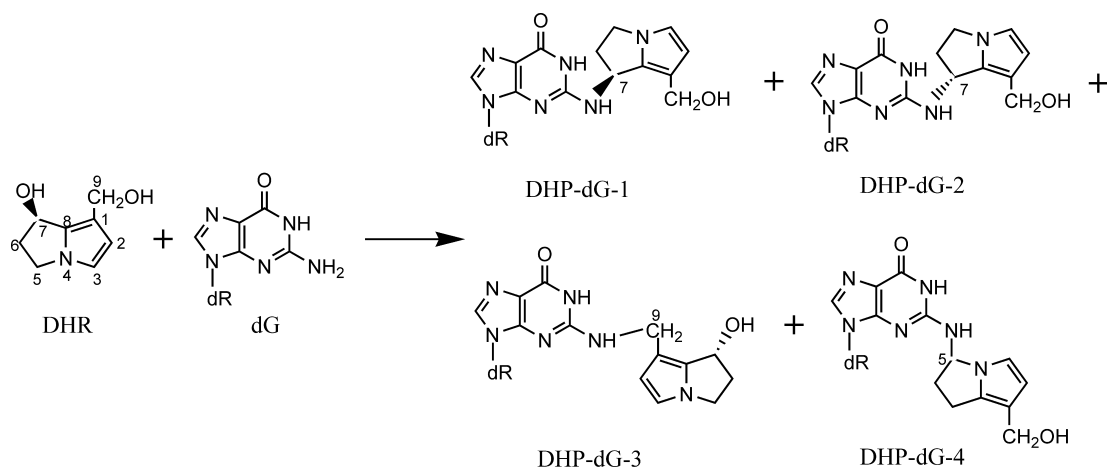
DHP-dA-2. ^1H NMR (DMSO- d_6 /D $_2$ O) δ 2.24–2.32 (1H, m, dA-H2''), 2.33–2.44 (1H, m, DHP-H6b), 2.62–2.74 (1H, m, dA-H2'), 2.85–2.96 (1H, m, DHP-H6a), 3.47–3.56 (1H, two sets of d, $J = 4.0$, dA-H5''), 3.65 (1H, m, dA-H5', overlapped with D $_2$ O), 3.84–3.92 (2H, m, DHP-H5b, dA-H4'), 4.02–4.23 (3H, m, DHP-H5a, H9a, H9b), 4.37–4.43 (1H, m, dA-H3'), 5.74 (1H, bs, DHP-H7), 6.03–6.09 (1H, two sets of d, $J = 2.0$, DHP-H2), 6.32–6.35 (1H, dd, dA-H1'), 6.60–6.65 (1H, two sets of d, $J = 2.0$, DHP-H3), 8.25 (1H, s, dA-H8), 8.32 (1H, s, dA-H2).

Synthesis of Isotopically Labeled DHP-dG and DHP-dA Adducts. DHP-[$^{15}\text{N}_5$]dG and DHP-[$^{15}\text{N}_5$, $^{13}\text{C}_{10}$]dA adducts were prepared as described above by reacting DHR (3.0 mg, 0.02 mmol) with [$^{15}\text{N}_5$]dG (5 mg, 0.02 mmol) and [$^{15}\text{N}_5$, $^{13}\text{C}_{10}$]dA (5 mg, 0.02 mmol), respectively.

Chemical Reaction of DHR with Calf Thymus DNA. To prepare DNA standards modified with DHR, 5 mg of calf thymus DNA in 2 mL of 5 mM Tris-HCl buffer, pH 7.1, containing 0.1 mM EDTA (Tris-EDTA) was reacted with 0, 0.1, 0.5, 1, 5, and 50 μg of DHR in 100 μL of methanol at 37 $^\circ\text{C}$ for 3 h. After the incubation, the reaction mixture was extracted twice with 5 mL of a chloroform/isoamyl alcohol mixture (24/1, v/v). The DNA in the aqueous phase was precipitated by adding 250 μL of 3 M sodium acetate followed by an equal volume of cold 2-propanol and washed with 70% ethanol. After the DNA was dissolved in Tris-EDTA, the DNA concentration was determined spectrophotometrically. The DNA solution was stored at -78 $^\circ\text{C}$ prior to hydrolysis and LC-ES-MS/MS analysis.

The deoxynucleoside adducts were quantified by HPLC-ES-MS/MS after standard enzymatic hydrolysis of the DNA to deoxynucleosides (43). The hydrolysis mixtures from 100 μg aliquots of the DHR-modified DNA were analyzed directly, without any adduct enrichment procedure.

HPLC-ES-MS/MS Analysis of DHP-Derived DNA Adducts Formed *in Vitro* and *in Vivo*. Quantification of DHP-DNA Standards. Purified samples of the DHP-dG-1 and DHP-dG2 adduct standards were quantified spectrophotometrically on the basis of the UV molar extinction coefficients 1.70×10^4 and 1.72×10^4

Scheme 1. Synthetic Preparation of DHP-dG Adducts^a

^a The absolute configuration assignments at the C7 positions of the necine base of DHP-dG-1 and DHP-dG-2 are arbitrary.

$M^{-1} \text{ cm}^{-1}$ at 256 nm (pH 7.0) reported by Robertson (44). DHP-dA-1 and DHP-dA-2 adduct standards were also quantified spectrophotometrically using the following experimentally determined UV molar extinction coefficients: $2.47 \pm 0.26 \times 10^4$ and $2.48 \pm 0.14 \times 10^4 M^{-1} \text{ cm}^{-1}$, respectively, at 271 nm in water and $2.21 \pm 0.23 \times 10^4$ and $2.18 \pm 0.12 \times 10^4 M^{-1} \text{ cm}^{-1}$, respectively, in methanol at 270 nm. The concentrations of the isotopically labeled adduct standards for DHP-dG-1, DHP-dG-2, DHP-dA-1, and DHP-dA-2 were quantified by LC-UV (256 nm) by comparison to the unlabeled standards. Isotopically labeled standards were not available for DHP-dG-3, DHP-dG-4, DHP-dA-3, and DHP-dA-4; isotopically labeled DHP-dG-2 was used as an internal standard for DHP-dG-3 and DHP-dG-4, and isotopically labeled DHP-dA-2 was used as an internal standard for DHP-dA-3 and DHP-dA-4. Response factors (i.e., unlabeled standard response/internal standard response) were determined by adding known amounts of labeled and unlabeled standards to DNA hydrolysates.

DNA Hydrolysis. DNA samples (typically $\sim 100 \mu\text{g}$) obtained from a reaction of DHR with calf thymus DNA, rats treated with riddelliine or monocrotaline, and rats from the NTP study were enzymatically hydrolyzed to nucleosides with micrococcal nuclease, spleen phosphodiesterase, and nuclease P1 as previously described (43). After adding approximately 50 fmol of each internal standard, the samples were injected on the HPLC for ES-MS/MS analyses.

Liquid Chromatography. The liquid handling system consisted of an Alliance 2795 separations module (Waters, Milford, MA), a Dionex GP40 quaternary gradient pump (Dionex, Sunnyvale, CA), and an automated switching valve (TPMV, Rheodyne, Cotati, CA). The switching valve allowed for online sample cleanup. The valve was used to divert the trap column effluent to either waste or to the analytical column. The Alliance 2795 system was used for sample injection, sample cleanup, and regeneration of the trap column. The Dionex pump was used to back-flush the trap column to the analytical column during analysis and to keep a constant flow of mobile phase going into the mass spectrometer during the sample loading and preparation periods.

Each sample was loaded onto a reverse phase trap column [Luna C18(2), $2 \text{ mm} \times 30 \text{ mm}$, $3 \mu\text{m}$, Phenomenex, Torrance, CA] with 95% water and 5% acetonitrile at a flow rate of 0.2 mL/min for 3.5 min. After switching the divert valve, the concentrated sample zone was back-flushed from the trap column onto the analytical column [Luna C18(2), $2 \text{ mm} \times 150 \text{ mm}$, $3 \mu\text{m}$, Phenomenex] with a water/acetonitrile gradient at 0.2 mL/min, and the sample components were eluted into the mass spectrometer. The gradient consisted of 10% acetonitrile for 2 min followed by a linear gradient up to 20% acetonitrile over 20 min, and then reset to the initial conditions. After 3 min, the valve was switched back to the load position, and the trap column was cleaned of waste with 70% of acetonitrile for 10 min at a flow rate of 0.5 mL/min. Then the trap

column was equilibrated with the starting mobile phase. The total run time for sample preparation and analysis was 34 min.

Mass Spectrometry. A Quattro Ultima quadrupole mass spectrometer (Waters, Milford, MA.), equipped with an ES interface, was used with a source block of 100°C and a desolvation temperature of 400°C . Nitrogen was the desolvation (750 L/h), cone gas (100 L/h), and nebulizing gas. Argon was the collision gas, at a collision cell pressure of 2.2×10^{-3} mBar. Positive ions were acquired in the multiple reaction monitoring (MRM) mode (dwell time of 0.2 s and interchannel delay of 0.03 s). The DHP-dG adducts were monitored at the $[(M + H)^+]$ (m/z 403) to m/z 269 transition and the dG internal standards at the $(M + H)^+$ (m/z 408) to m/z 274 transition. The DHP-dA adducts were monitored at the $[(M + H)^+]$ (m/z 387) to m/z 253 transition and the dA internal standards at the $(M + H)^+$ (m/z 402) to m/z 263 transition. The cone voltage was 25 V, and the collision energy was 14 eV for all of the transitions. Samples were quantified by comparing the areas of the unlabeled chromatogram peaks to those of the corresponding labeled internal standard chromatogram peaks.

Results

Synthesis of DHP-dG Adducts. DHP-dG adducts were synthesized by the reaction of DHR with dG (Scheme 1). The resulting reaction products were purified by HPLC, first with a Whatman ODS-3 column, to remove excess dG (data not shown), and then with a Prodigy $5 \mu\text{m}$ ODS column (Figure 3A). The materials contained in the chromatographic peaks eluted at 18.2 (DHP-dG-1) and 19.5 (DHP-dG-2) min showing baseline separation and exhibited UV-visible absorption spectra (Figure 4A) that were identical to those reported by Robertson (44). The whole scan mass spectra of these compounds revealed that both had protonated molecules $(M + H)^+$ at m/z 403 (data not shown). These products were also characterized by ES/MS positive product ion spectra, which showed transition ions at m/z 269 (DHP-guanine-OH), m/z 152 (guanine), and m/z 136 (DHP) (Figure 5).

The CD spectra of DHP-dG-1 and DHP-dG-2 were similar to those reported by Robertson (44). The CD Cotton effects of DHP-dG-1 were approximate mirror images of those of DHP-dG-2 (Figure 6A), indicating that these adducts were a pair of epimers differing in the configuration of the stereocenter of the DHR chromophore. The ^1H NMR spectra of DHP-dG-1 and DHP-dG-2 showed characteristic downfield shifts (ca. 0.27 ppm) of H7 compared to H7 in DHR itself (Table 1), as reported by Robertson (44). By contrast, the location of the resonances for H2, H3, H5a, H5b, H9a, and H9b showed smaller downfield

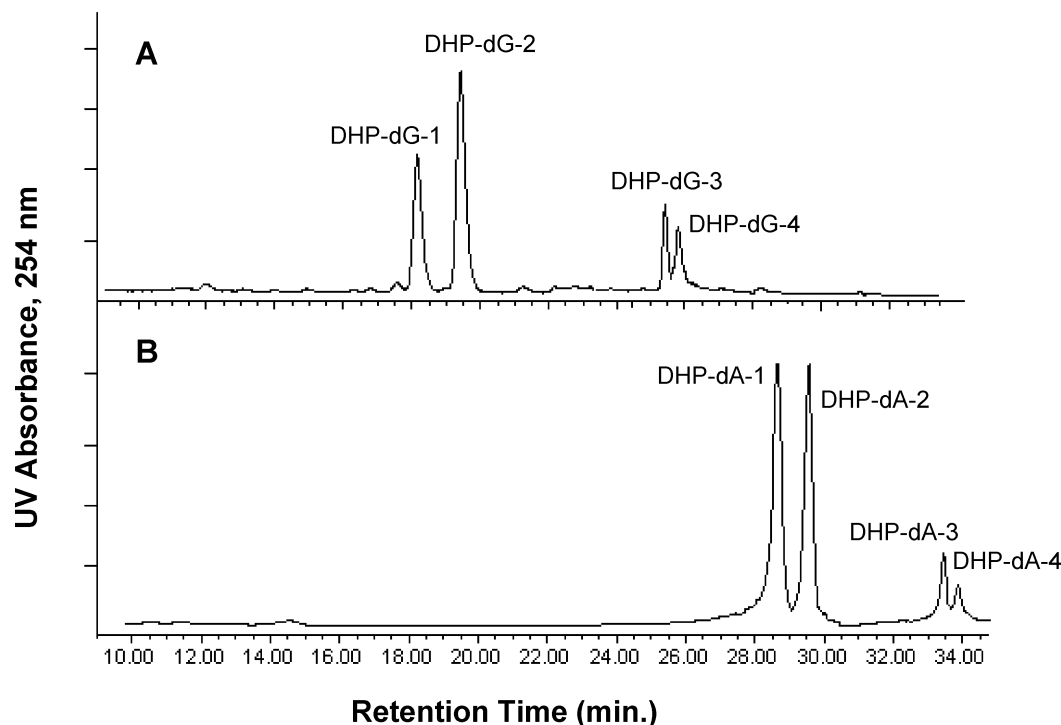


Figure 3. Reversed-phase HPLC profiles of (A) DHP-dG adducts and (B) DHP-dA adducts formed from reactions of DHR with 2'-deoxyguanosine (dG) and 2'-deoxyadenosine (dA), respectively. For HPLC conditions, see Experimental Procedures.

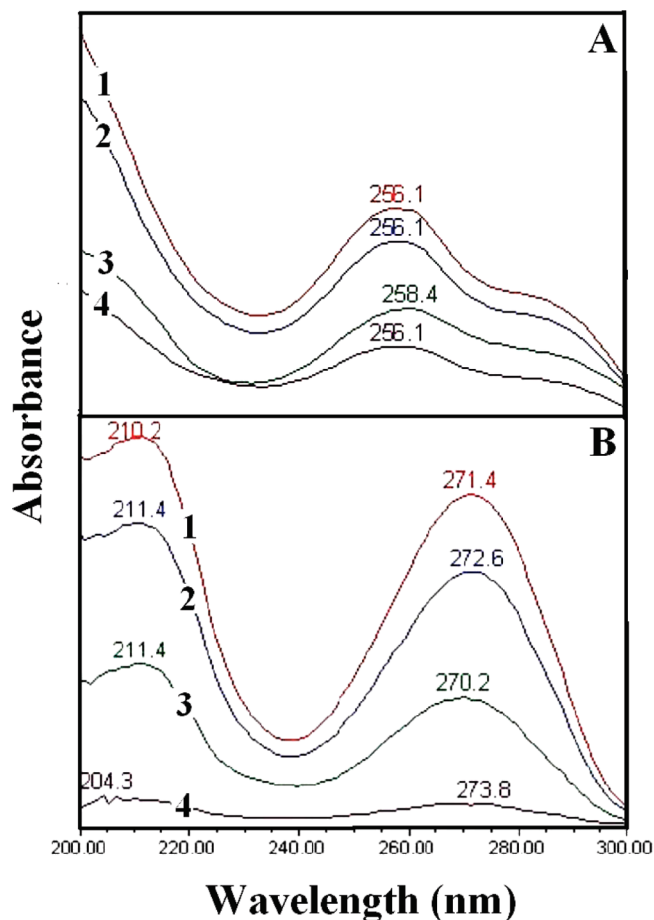


Figure 4. UV-visible absorption spectra of (A) 1, DHP-dG-1; 2, DHP-dG-2; 3, DHP-dG-3; and 4, DHP-dG-4; and (B) 1, DHP-dA-1; 2, DHP-dA-2; 3, DHP-dA-3; and 4, DHP-dA-4. Spectra were obtained in 25% methanol in water.

shifts from the same resonances in DHR. Moreover, both geminal H6 protons were substantially deshielded (ca. 0.18–0.26

ppm) compared to the corresponding protons in DHR, which indicated proximity to the substitution site. These data were consistent with adduct formation through substitution at H7 of the DHP moiety. Each of the deoxyribose protons was clearly evident in both DHP-dG-1 and DHP-dG-2. In addition, resonances could be assigned to H8 and N1H of dG, which excluded substitution at C8, N1, or O⁶ of the dG moiety. On the basis of the UV-visible absorption, mass, CD, and NMR spectra, the structures of DHP-dG-1 and DHP-dG-2 were characterized as a pair of epimeric DHP-dG adducts in which reaction had occurred between C7 of DHP and N² of dG (i.e., (±)-7-(deoxyguanosin-N²-yl)dehydrocupinidine) (Scheme 1).

The materials eluting at 25.5 (DHP-dG-3) and 25.8 (DHP-dG-4) min (Figure 3A) had UV-visible absorption spectra (Figure 4A) identical to those of DHP-dG-1 and DHP-dG-2. Whole scan mass spectra revealed that the adducts had protonated molecules (M + H)⁺ at *m/z* 403 (data not shown). Similar to the mass spectrometric pattern of DHP-dG-1 and DHP-dG-2, product ion mode mass spectrometric analysis indicated that both DHP-dG-3 and DHP-dG-4 had transition ions at *m/z* 269 (DHP-guanine-OH), *m/z* 152 (guanine), and *m/z* 136 (DHP) (Figure 5).

In contrast to DHP-dG-1 and DHP-dG-2, the ¹H NMR spectrum of DHP-dG-3 had a resonance for H7 of the DHP moiety that was nearly identical to H7 of DHR (Table 1 and Figure 7); likewise, H2, H3, and both pairs of geminal H5 and H6 protons were almost unaffected by adduct formation. In addition, both H9a and H9b appeared as a set of mutually coupled doublets (Table 1), which suggested significant prochirality. As with DHP-dG-1 and DHP-dG-2, resonances could be assigned to each of the deoxyribose protons, H8, and N1H of dG. These NMR data indicated that reaction had occurred at C9 of DHR through the exocyclic nitrogen of dG, an interpretation supported by a fragment at *m/z* 164 in the product ion mass spectrum, which is consistent with a protonated guanine bearing a methylene group at the N² position. Thus, on the basis of the UV-visible, mass, and

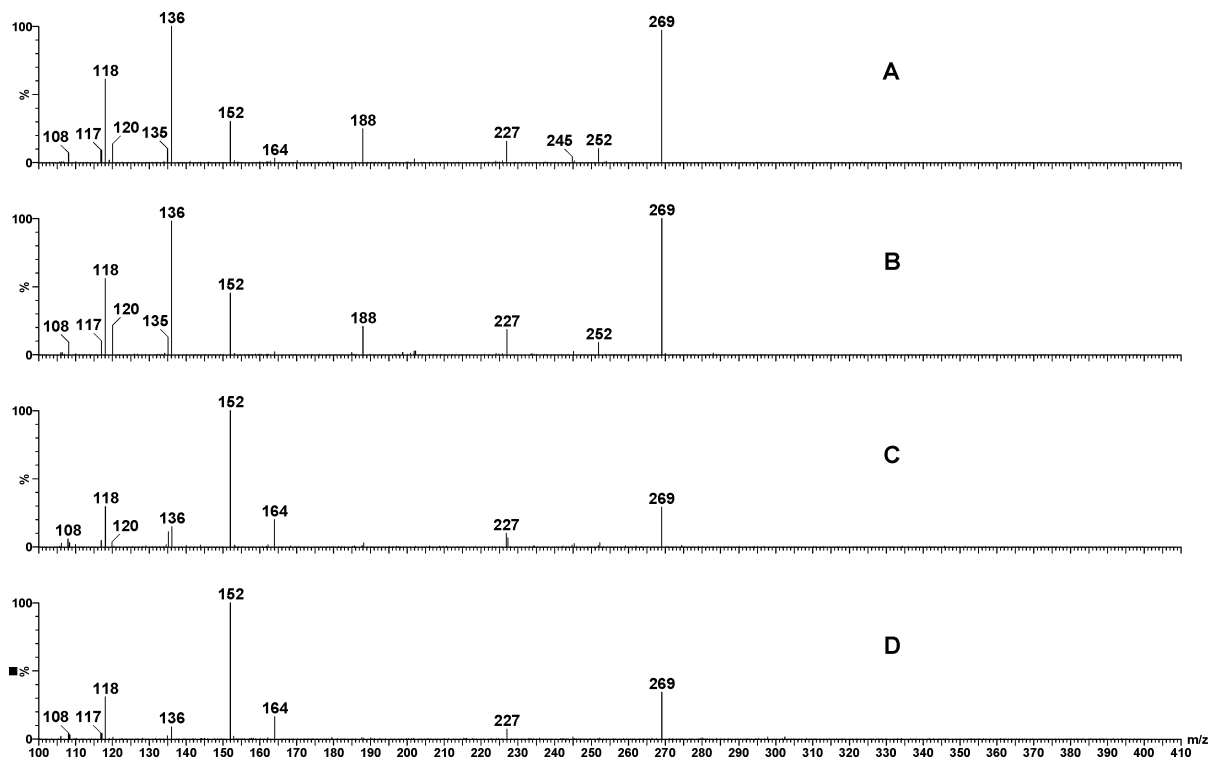


Figure 5. Electrospray positive product ion mass spectra of the four DHP-dG adduct standards (A = DHP-dG-1, B = DHP-dG-2, C = DHP-dG-3, and D = DHP-dG-4). The product ions of the $(M + H)^+$ m/z 403 were acquired with a cone voltage of 25 V and a collision energy of 30 eV.

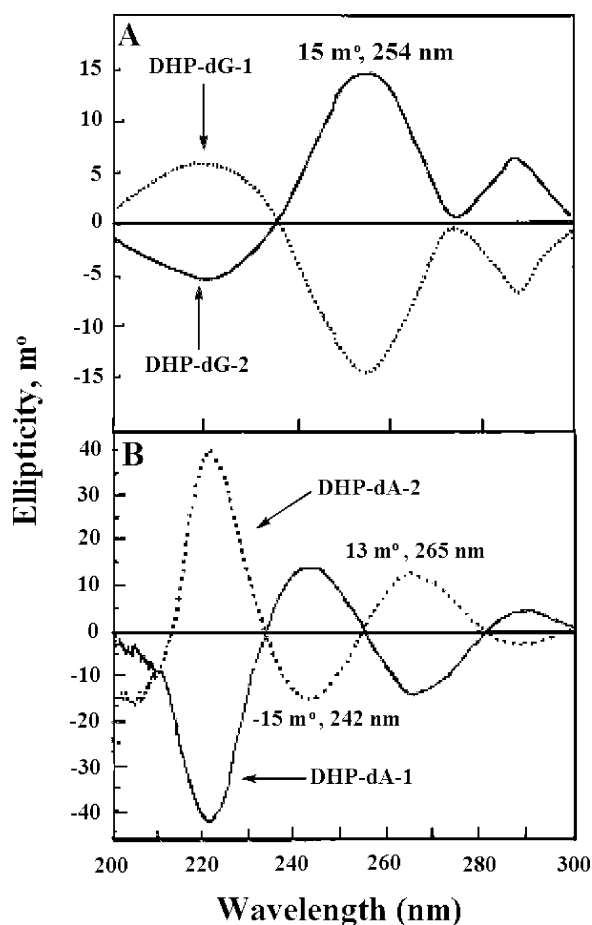


Figure 6. CD spectra of (A) DHP-dG-1 and DHP-dG-2 in methanol, and (B) DHP-dA-1 and DHP-dA-2 in water.

^1H NMR spectroscopic data, DHP-dG-3 was characterized as 9-(deoxyguanosin- N^2 -yl)dehydrosupinidine (Figure 7).

The ^1H NMR spectrum of DHP-dG-4 had a single C-5 proton, which was shifted downfield by approximately 0.8–1 ppm relative to H5 in DHR and the other DHP-dG adducts (Table 1 and Figure 7). In contrast to the other adducts, there were two H7 resonances in DHP-dG-4, and these were shifted upfield by approximately 1–1.3 ppm compared to that of the H7 resonance in DHR and the other DHP-dG adducts. As with the other DHP-dG adducts, resonances were clearly evident for each of the deoxyribose protons, H8, and N1H of dG. Thus, on the basis of its UV–visible, mass, and ^1H NMR spectroscopic data, DHP-dG-4 was characterized as 5-(deoxyguanosin- N^2 -yl)dehydrosupinidine.

The UV molar extinction coefficients of DHP-dG-1 and DHP-dG-2 were previously reported by Robertson (44). On the basis of the similarity of the UV spectra (Figure 4A) and assuming that the molar extinction coefficients of DHP-dG-3 and DHP-dG-4 are identical to those of DHP-dG-1 and DHP-dG-2, the yields of these four adducts in the crude reaction mixture of DHR with dG were estimated from the corresponding HPLC peak areas as follows: DHP-dG-1, 0.89%; DHP-dG-2, 0.69%; DHP-dG-3, 0.15%; and DHP-dG-4, 0.06%. Because of the unstable nature of pyrrolic compounds, these adducts, particularly DHP-dG-3 and DHP-dG-4, decomposed during HPLC purification.

Synthesis of DHP-dA Adducts. DHP-dA adducts were synthesized by the reaction of DHR with dA (Scheme 2) and purified by HPLC, first with a Whatman ODS-3 column (not shown) and then with a Prodigy 5 μm ODS column (Figure 3B). Whole scan mass spectrometric analysis revealed that the materials contained in the chromatographic peaks eluted at 28.5 (DHP-dA-1), 29.5 (DHP-dA-2), 33.4 (DHP-dA-3), and 33.9 (DHP-dA-4) min had protonated molecules $(M + H)^+$ at m/z 387 (data not shown); electrospray positive product ion mass spectrometric analysis indicated transition ions at m/z 253 (DHP-adenine-OH) and m/z 136 (DHP) (Figure 8), which suggested that they were DHP-dA adducts.

Table 1. Proton NMR Spectroscopic Data (500 MHz) of DHP Protons in the Synthetically Prepared DHP-dG and DHP-dA Adducts Measured in DMSO- d_6 /D $_2$ O a

assignment	adduct						
	DHR	DHP-dG-1	DHP-dG-2	DHP-dG-3	DHP-dG-4	DHP-dA-1	DHP-dA-2
H6b	2.15–2.20 (1H, m)	2.31–2.37 (1H, m)	2.34–2.36 (1H, m)	2.18–2.25 (1H, m)	2.34–2.39 (1H, m)	2.33–2.47 (1H, m)	2.33–2.44 (1H, m)
H6a	2.57–2.65 (1H, m)	2.83–2.90 (1H, m)	2.83–2.90 (1H, m)	2.55–2.66 (1H, m)	2.56–2.65 (1H, m)	2.87–2.96 (1H, m)	2.85–2.96 (1H, m)
H5b	3.75–3.79 (1H, m)	3.87–3.91 (1H, m)	3.87–3.92 (1H, m)	3.78–3.83 (1H, m)		3.84–3.92 (1H, m)	3.84–3.92 (1H, m)
H5a	3.94–3.98 (1H, m)	3.99–4.03 (1H, m)	4.00–4.03 (1H, m)	3.98–4.03 (1H, m)		4.04–4.23 (1H, m)	4.02–4.23 (1H, m)
H5					4.74 (1H, dd, $J = 6.4, 7.6$)		
H9b	4.27 (1H, d, $J = 12$)	4.25 (1H, d, $J = 12$)	4.26 (1H, d, $J = 12$)	4.24 (1H, two sets of d, $J = 14$)	4.26 (1H, t, $J = 14$)	4.04–4.23 (1H, m)	4.02–4.23 (1H, m)
H9a	4.33 (1H, d, $J = 12$)	4.29 (1H, d, $J = 12$)	4.30 (1H, d, $J = 12$)	4.32 (1H, two sets of d)	4.35 (1H, two sets of d, $J = 14.2$)	4.04–4.23 (1H, m)	4.02–4.23 (1H, m)
H7	4.99 (1H, dd, $J = 6.5, 2.5$)	5.25–5.27 (1H, m)	5.25–5.27 (1H, m)	5.03–5.08 (1H, m)		5.72 (1H, bs)	5.74 (1H, bs)
H7b					3.84–3.90 (1H, m)		
H7a					3.92–3.97 (1H, m)		
H2	6.02 (1H, d, $J = 2.5$)	6.08 (1H, d, $J = 2.5$)	6.08 (1H, d, $J = 2.5$)	6.07 (1H, d, $J = 2.7$)	6.11 (1H, d, $J = 2.7$)	6.04–6.06 (1H, two sets of d, $J = 2.5$)	6.03–6.09 (1H, d, $J = 2.0$)
H3	6.54 (1H, d, $J = 2.6$)	6.65 (1H, d, $J = 2.5$)	6.65 (1H, d, $J = 2.5$)	6.60 (1H, d, $J = 2.5$)	6.68 (1H, two sets of d, $J = 2.7$)	6.59–6.65 (1H, two sets of d, $J = 2.5$)	6.60–6.65 (1H, two sets of d, $J = 2.0$)

^a Because of insufficient materials of DHP-dA-3 and DHP-dA-4, NMR spectroscopic analysis was not possible.

DHP-dA-1 and DHP-dA-2 had identical UV–visible absorption spectra (Figure 4B) and highly similar ^1H NMR spectra (Figure 9). As shown in Figure 6B, the CD Cotton effects of DHP-dA-1 were an approximate mirror image of those of DHP-dA-2, indicating that these adducts were a pair of epimers differing in the configuration of one stereocenter in the DHR chromophore. Similar to DHP-dG-1 and DHP-dG-2, the ^1H NMR spectra of DHP-dA-1 and DHP-dA-2 showed characteristic downfield shifts (ca. 0.73 ppm) of H7 compared to that of H7 in DHR (Figure 9 and Table 1). Resonances could be assigned to H2, H3, H5a, H5b, H6a, H6b, H9a, and H9b. With the exception of H9a and H9b, which were shielded by approximately 0.2 ppm, these resonances were very similar to those observed for DHP-dG-1 and DHP-dG-2. These data are consistent with substitution through C7 of the DHR moiety, with positioning of the methylene C9 protons in the shielding zone of the adenine ring. Each of the deoxyribose protons was clearly evident for the dA moiety. In addition, resonances could be assigned to H2 and H8, and the N^6H resonance appeared as a single proton. On the basis of the UV–visible absorption, mass, CD, and NMR spectra, the structures of DHP-dA-1 and DHP-dA-2 were characterized as a pair of epimeric DHP-dA adducts in which the reaction had occurred between C7 of DHP and N^6 of dA [i.e., (\pm)-7-(deoxyadenosin- N^6 -yl)dehydrosupinidine] (Scheme 2).

There was an insufficient amount of material for ^1H NMR spectroscopic characterization of DHP-dA-3 and DHP-dA-4. On the basis of their mass and UV–visible spectroscopic characteristics, DHP-dA-3 and DHP-dA-4 were tentatively assigned as dA-dehydrosupinidine adducts. With the assumption that DHP-dA-3 and DHP-dA-4 have molar extinction coefficients similar to those of DHP-dA-1 and DHP-dA-2, upon HPLC analysis, the crude yields of these adducts were estimated as follows: DHP-dA-1, 0.1%; DHP-dA-2, 0.1%; DHP-dA-3, 0.01%; and DHP-dA-4, 0.01%.

Synthesis of Isotopically Labeled DHP-[$^{15}\text{N}_5$]dG and DHP-[$^{15}\text{N}_5$, $^{13}\text{C}_{10}$]-dA. DHP-[$^{15}\text{N}_5$]dG and DHP-[$^{15}\text{N}_5$, $^{13}\text{C}_{10}$]dA adducts were similarly prepared by reacting DHR with [$^{15}\text{N}_5$]dG and [$^{15}\text{N}_5$, $^{13}\text{C}_{10}$]dA, respectively. DHP-[$^{15}\text{N}_5$]dG-1, DHP-[$^{15}\text{N}_5$]dG-2, DHP-[$^{15}\text{N}_5$]dG-3, and DHP-[$^{15}\text{N}_5$]dG-4 showed a ($\text{M} + \text{H}$) $^+$ at m/z 408 and a transition ion at m/z 274 (DHR-[$^{15}\text{N}_5$]guanine-OH) (data not shown). DHP-[$^{15}\text{N}_5$, $^{13}\text{C}_{10}$]dA-1, DHP-[$^{15}\text{N}_5$, $^{13}\text{C}_{10}$]dA-2, DHP-[$^{15}\text{N}_5$, $^{13}\text{C}_{10}$]dA-3, and DHP-[$^{15}\text{N}_5$, $^{13}\text{C}_{10}$]dA-4 had a ($\text{M} + \text{H}$) $^+$ at m/z 402 and a transition ion at m/z 263 (data not shown).

Standard Characterization and Calibration Curves. HPLC-ES-MS/MS calibration curves were generated for synthetically prepared DHP-dG-1, DHP-dG-2, DHP-dA-1, and DHP-dA-2 versus their respective [$^{15}\text{N}_5$] and [$^{15}\text{N}_5$, $^{13}\text{C}_{10}$] internal standards. Response factors were generated from these curves. The curves for the unlabeled compounds went from 10 to 500 fmol on-column versus 50 fmol of the [$^{15}\text{N}_5$] and [$^{15}\text{N}_5$, $^{13}\text{C}_{10}$] internal standards. The curves were linear with $r^2 > 0.999$.

[$^{15}\text{N}_5$] adduct standards did not exist for DHP-dG-3, DHP-dG-4, DHP-dA-3, and DHP-dA-4. To generate response factors for these adducts, 100 μg aliquots of hydrolyzed DNA were fortified with the following mixtures: 50 fmol DHP-dG-3 and 55 fmol DHP-[$^{15}\text{N}_5$]dG-2; 25 fmol DHP-dG-4 and 55 fmol DHP-[$^{15}\text{N}_5$]dG-2; 50 fmol DHP-dA-3 and 82 fmol DHP-[$^{15}\text{N}_5$, $^{13}\text{C}_{10}$]dA-2; and 134 fmol DHP-dA-4 and 82 fmol DHP-[$^{15}\text{N}_5$, $^{13}\text{C}_{10}$]dA-2. The final response factors obtained were as follows: DHP-dG-1 vs DHP-[$^{15}\text{N}_5$]dG-1 = 1.18; DHP-dG-2 vs DHP-[$^{15}\text{N}_5$]dG-2 = 1.20; DHP-dG-3 vs DHP-[$^{15}\text{N}_5$]dG-2 = 2.10; DHP-dG-4 vs DHP-[$^{15}\text{N}_5$]dG-2 = 1.50; DHP-dA-1 vs DHP-

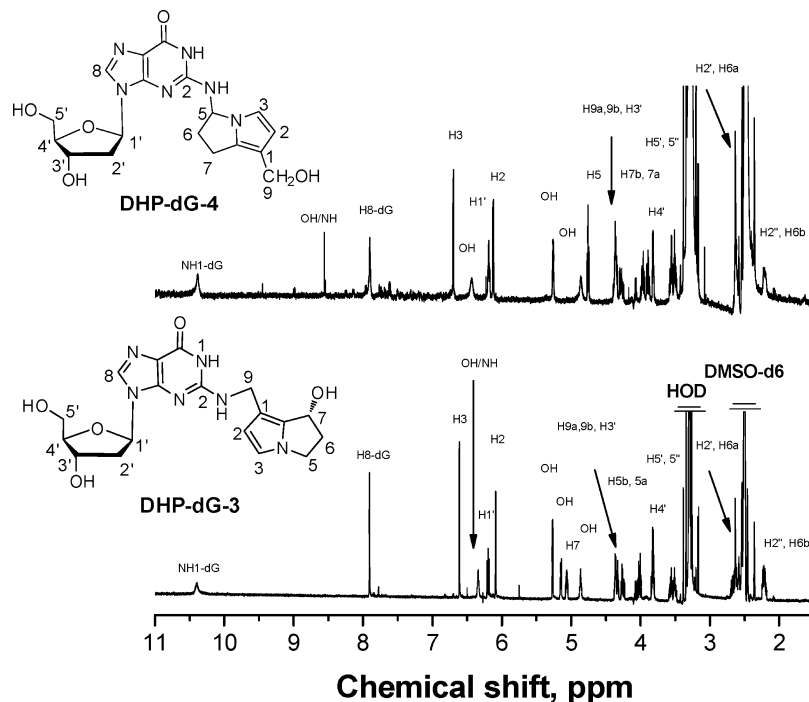
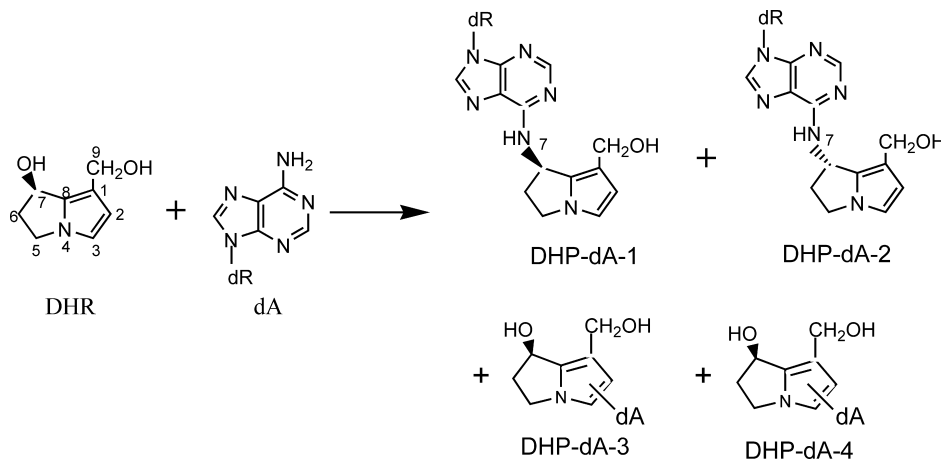


Figure 7. ^1H NMR spectra of DHP-dG-3 and DHP-dG-4 measured in $\text{DMSO-}d_6$.

Scheme 2. Synthetic Preparation of DHP-dA Adducts^a



^a The absolute configuration assignments at the C7 positions of the necine base of DHP-dA-1 and DHP-dA-2 are arbitrary.

$^{15}\text{N}_5$, $^{13}\text{C}_{10}$]dA-1 = 0.93; DHP-dA-2 vs DHP- $^{15}\text{N}_5$, $^{13}\text{C}_{10}$]dA-2 = 0.91; DHP-dA-3 vs DHP- $^{15}\text{N}_5$, $^{13}\text{C}_{10}$]dA-2 = 6.50; and DHP-dA-4 vs DHP- $^{15}\text{N}_5$, $^{13}\text{C}_{10}$]dA-2 = 4.2.

HPLC-ES-MS/MS Analysis of DHP-dG and DHP-dA Adducts Formed from the Reaction of Calf Thymus DNA and DHR. DHP-DNA adducts were prepared by reactions of 5 mg of calf thymus DNA in 2 mL of 5 mM Tris-HCl buffer, pH 7.1, containing 0.1 mM EDTA with 0, 0.1, 0.5, 1, 5, and 50 μg of DHR in 100 μL of methanol at 37 $^\circ\text{C}$ for 3 h. After enzymatic hydrolysis of the resulting reaction mixtures, the quantity of DHP-dG and DHP-dA adducts in each reaction was determined by HPLC-ES-MS/MS through multiple reaction monitoring (MRM) combined with the use of DHP- $^{15}\text{N}_5$]dG and DHP- $^{15}\text{N}_5$, $^{13}\text{C}_{10}$]dA adducts as internal standards. Representative multiple reaction monitoring (MRM) measurements for DHP-dG and DHP-dA adducts formed by reacting 5 mg of calf thymus DNA with 5 μg of DHR are shown in Figure 10, which clearly indicates the presence of all four DHP-dG and DHP-dA adducts.

The levels of DHP-dG and DHP-dA adducts formed from each of the reactions are tabulated in Table 2. These results indicate that (i) DHP-dG and DHP-dA adducts were formed in a dose-responsive manner; (ii) DHP-dA-3 and DHP-dA-4 were the most abundant, followed by all of the DHP-dG adducts, which were formed to a similar extent, and DHP-dA-1 and DHP-dA-2 were formed to the least extent; and (iii) DHP-dA and DHP-dG adducts could be detected even at the lowest treatment group (0.1 μg of DHR reacted with 5 mg of calf thymus DNA).

HPLC-ES-MS/MS Analysis of DHR-dG and DHR-dA Adducts Formed *in Vivo*. Female rats were dosed daily with riddelliine (0.1, 1.0, 2.0, and 5.0 mg/kg body weight) or monocrotaline (1.0 and 5.0 mg/kg body weight) for three consecutive days. One day after the last treatment, DNA was isolated from the livers for the analysis of DHP-dG and DHP-dA adducts by HPLC-ES-MS/MS. Representative MRM chromatograms of liver DNA from a rat dosed with 5 mg of monocrotaline/kg body weight/day and a rat dosed with 5 mg of riddelliine/kg body weight/day are shown in Figure

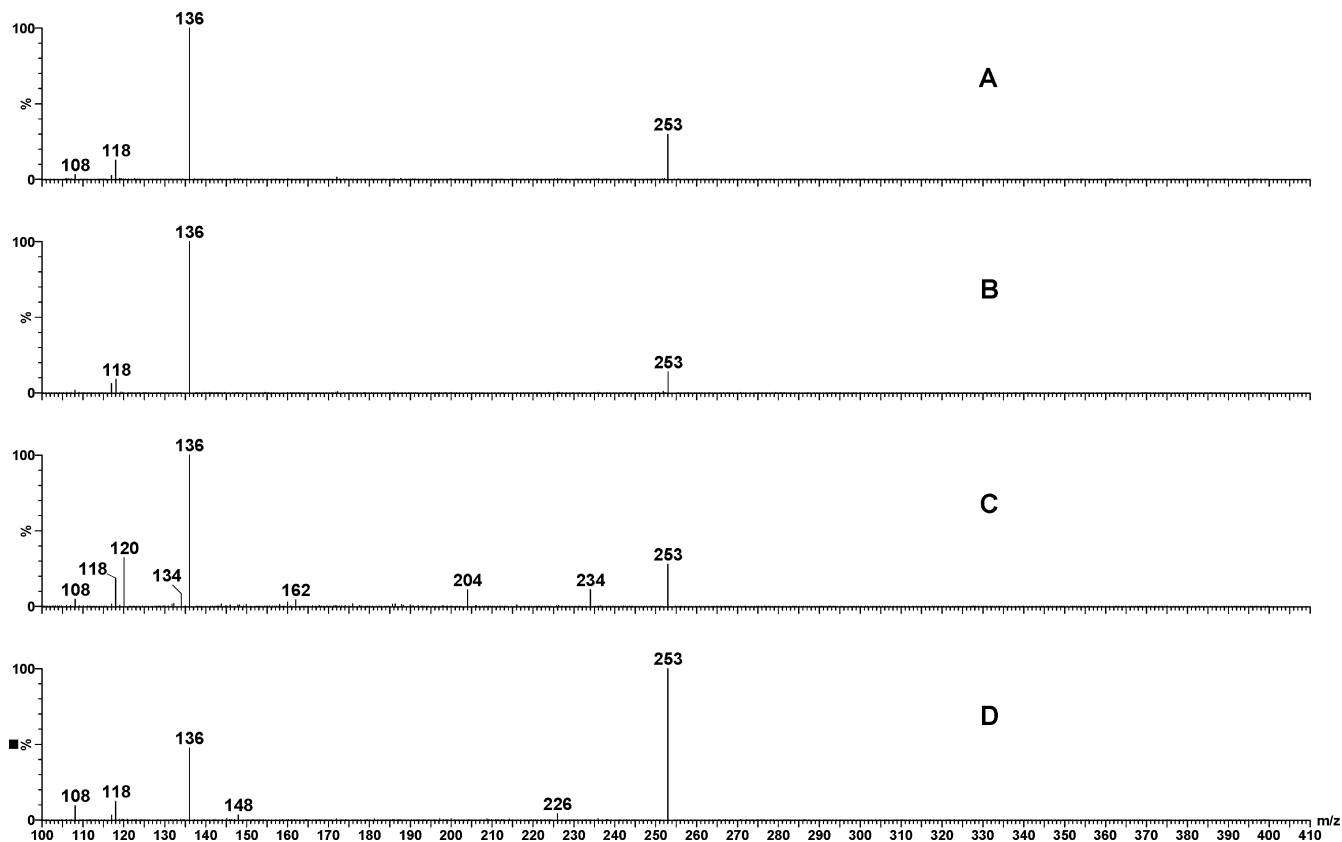


Figure 8. Electrospray positive product ion mass spectra of the four DHP-dA adduct standards (A = DHP-dA-1, B = DHP-dA-2, C = DHP-dA-3, and D = DHP-dA-4). The product ions of the MH^+ m/z 387 were acquired with a cone voltage of 25 V and a collision energy of 30 eV.

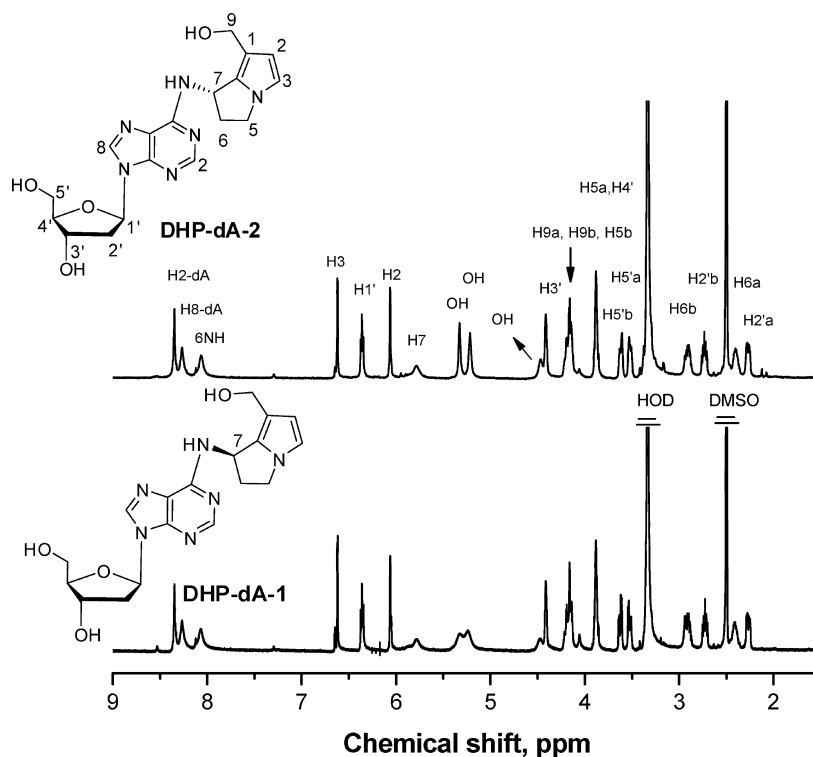


Figure 9. 1H NMR spectra of DHP-dA-1 and DHP-dA-2 measured in $DMSO-d_6$.

11. The data, which are summarized in Table 3, indicate that for both riddelliine and monocrotaline (i) DHP-dG-3 and DHP-dG-4 were formed in a dose-responsive manner and to a greater extent than DHP-dA-3 and DHP-dA-4; and that (ii) with the exception of DHP-dA-2, which was found in liver DNA from rats treated with 5 mg of riddelliine/kg body

weight/day, DHP-dG-1, DHP-dG-2, DHP-dA-1, and DHP-dA-2 were not detected in any treatment groups.

HPLC-ES-MS/MS Analysis of DHP-dG and DHP-dA Adducts Formed in Rat Liver Samples from an NTP Study. In a previous study, we used the ^{32}P -postlabeling methodology to determine the levels of DHP-derived DNA

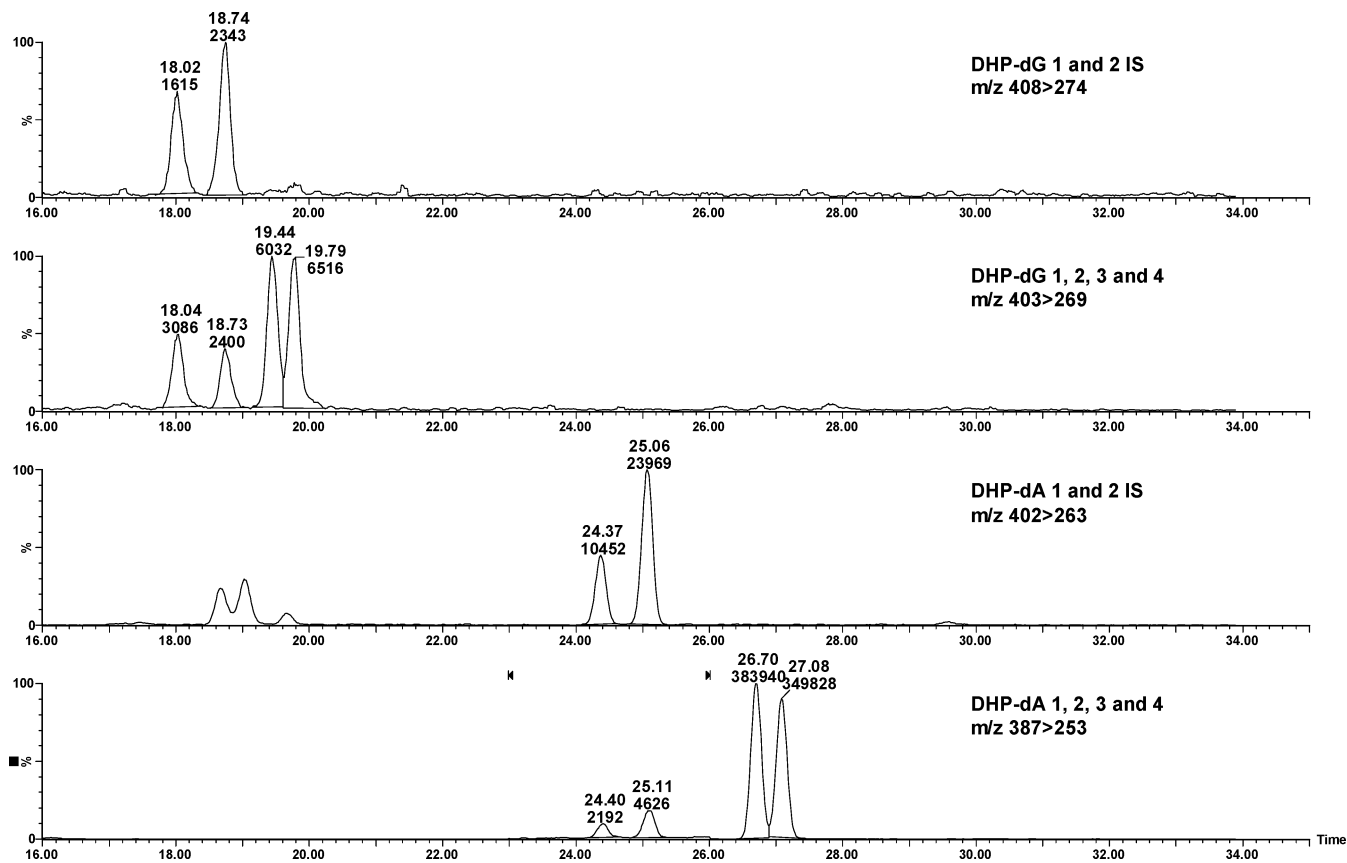


Figure 10. Representative MRM chromatograms (relative signal intensity vs time) for DHP-dG and DHP-dA adducts formed during the *in vitro* reaction of 5 mg of calf thymus DNA with 5 μg of DHR. Internal standards (IS) were added in amounts of 50, 55, 50, and 80 fmol for DHP-dG-1, DHP-dG-2, DHP-dA-1, and DHP-dA-2, respectively.

Table 2. Levels of DHP-dG and DHP-dA Adducts Formed from Reactions of 5 mg of Calf Thymus DNA in 2 mL of 5 mM Tris-HCl Buffer, pH 7.1, Containing 0.1 mM EDTA and 0, 0.1, 0.5, 1, 5, or 50 μg of DHR in 100 μL of Methanol for 3 h

sample	levels of DHP-dG and DHP-dA/ 10^8 nucleotides							
	DHP-dG-1	DHP-dG-2	DHP-dG-3	DHP-dG-4	DHP-dA-1	DHP-dA-2	DHP-dA-3	DHP-dA-4
50 μg	213.5	164.6	143.0	180.6	20.1	21.9	266.0	366.0
5 μg	24.6	15.5	23.0	30.1	2.3	3.5	42.7	60.7
1 μg	15.3	10.4	19.4	23.1	1.9	3.0	27.3	37.8
0.5 μg	<LOD	<LOD	5.4	5.8	<LOD	0.3	4.4	6.3
0.1 μg	<LOD	<LOD	1.3	<LOD	<LOD	<LOD	1.2	1.6
0 μg	<LOD	<LOD	<LOD	<LOD	0.3	0.1	<LOD	<LOD
LOD ^b	1.5	1.5	1.2	1.5	0.1	0.1	0.1	0.1

^a The reaction consisted of the amount of DHR indicated in the presence of 5 mg of DNA. ^b LOD = limit of detection based upon the analysis of 100 μg of DNA by HPLC-ES-MS/MS.

adducts in liver samples from an NTP study in which female F344 rats were treated with riddelliine for six months (41). In the current study, we assessed the same samples by HPLC-ES-MS/MS. Representative chromatograms are shown in Figure 12, and the data are summarized in Table 4. As with the DNA samples from the rats treated for three days with either riddelliine or monocrotaline, DHP-dG-3- and DHP-dG-4 were formed in a dose-responsive manner and to a greater extent than DHP-dA-3 and DHP-dA-4. Likewise, DHP-dG-1, DHP-dG-2, DHP-dA-1, and DHP-dA-2 were not detected in any treatment groups.

Discussion

Pyrrolizidine alkaloids are a class of genotoxic and tumorigenic naturally occurring phytochemicals (3–6, 8, 26). In this article, we report the development of a sensitive HPLC-ES-MS/MS method for the detection of DHP-derived DNA adducts and the utilization of this method for the detection and quantification of these adducts from *in vitro* and *in vivo* samples.

To develop the method, the eight DHP-dG and DHP-dA adducts, namely, DHP-dG-1, DHP-dG-2, DHP-dG-3, DHP-dG-4, DHP-dA-1, DHP-dA-2, DHP-dA-3, and DHP-dA-4, as well as their [¹⁵N₅]dG and [¹⁵N₅, ¹³C₁₀]dA adducts, were prepared synthetically. Upon determination of the optimal HPLC and mass spectrometric conditions, we are able to detect these eight DHP-derived dG and dA adducts *in vitro* and/or *in vivo* and quantify the formation of these adducts in the multiple reaction monitoring (MRM) mode. The DNA adducts assessed included those formed from the reaction of DHR with calf thymus DNA *in vitro*, in liver DNA from female rats treated with different doses of riddelliine or monocrotaline for three consecutive days, and in liver DNA from female rats treated with riddelliine for six months.

In this developed HPLC-ES-MS/MS method, the sensitivity for different DHP-DNA adducts varies in the range of 0.1–1.5 adducts in 10^8 nucleotides for the analysis of 100 μg samples. This level of sensitivity is potentially adequate for measuring

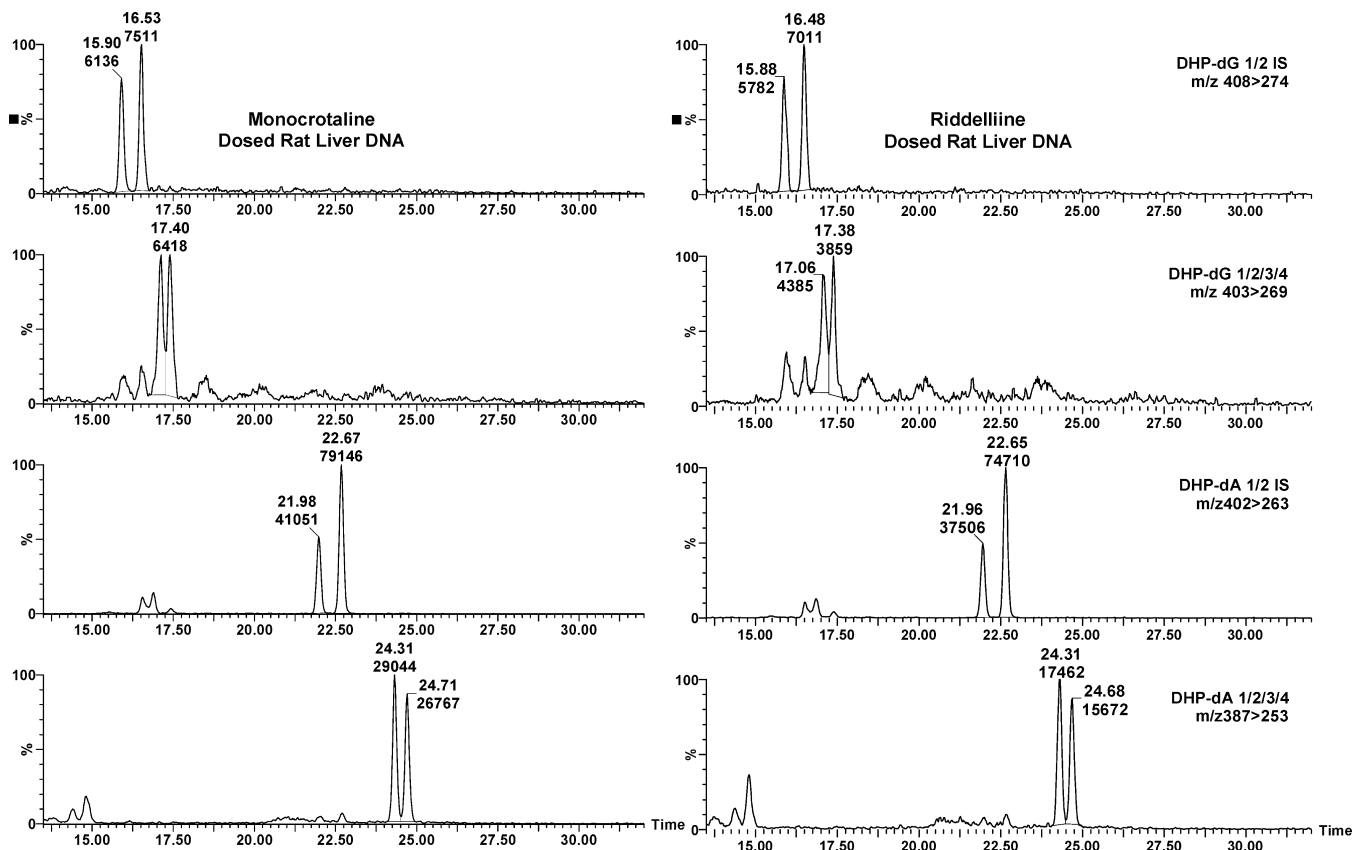


Figure 11. Representative MRM chromatograms (relative signal intensity vs time) for rat liver DNA samples. The right panels show a 100 μ g aliquot of DNA from a rat dosed daily with 5 mg of riddelliine/kg body weight for three days, and the left panels show a 100 μ g sample of DNA from a rat dosed daily with 5 mg of monocrotaline/kg body weight for three days. Internal standards (IS) were added in amounts of 50, 55, 50, and 80 fmol for DHP-dG-1, DHP-dG-2, DHP-dA-1, and DHP-dA-2, respectively.

Table 3. Levels of DHP-dG and DHP-dA Adducts Formed in the Livers of Female Rats Dosed with Riddelliine or Monocrotaline for Three Consecutive Days

treatment (mg/kg body weight/day)	levels of DHP-dG and DHP-dA/10 ⁸ nucleotides ^a							
	DHP-dG-1	DHP-dG-2	DHP-dG-3	DHP-dG-4	DHP-dA-1	DHP-dA-2	DHP-dA-3	DHP-dA-4
	riddelliine							
5	<LOD	<LOD	7.5	10.2	<LOD	0.5	1.0	1.4
2	<LOD	<LOD	5.0	4.9	<LOD	<LOD	0.5	0.6
1	<LOD	<LOD	2.0	2.6	<LOD	<LOD	0.3	0.3
0.1	<LOD	<LOD	<LOD	<LOD	<LOD	<LOD	0.1	0.1
	monocrotaline							
5	<LOD	<LOD	5.2	6.9	<LOD	<LOD	0.6	0.9
1	<LOD	<LOD	<LOD	<LOD	<LOD	<LOD	0.1	0.1
	control							
	<LOD	<LOD	<LOD	<LOD	<LOD	<LOD	<LOD	<LOD

^a Aliquots of DNA (100 μ g) were assayed by HPLC-ES-MS/MS. The LOD for each of the adducts is given in Table 2.

adduct levels in exposed humans, provided that sufficient DNA samples can be collected (e.g., lymphocyte DNA is present in whole blood at 6 μ g/mL), that the ingested doses are high enough (e.g., detectable in rat liver from 3 doses of 0.1 mg/kg bw riddelliine), and that samples are collected soon enough after ingestion so that adduct loss through DNA repair does not occur.

There were marked differences in regioselectivity depending upon the system being investigated. Reactions of DHR with dG produced a pair of epimeric DHP-dG-1 and DHP-dG-2 as the predominant adducts, with DHP-dG-3 and DHP-dG-4 being formed in a much lower yield (Figure 3A). Likewise, DHR reacted with dA in a regioselective manner to produce predominantly DHP-dA-1 and DHP-dA-2 (Figure 3B). When DHR was reacted with calf thymus DNA, all four DHP-dG adducts were formed to a similar but to a lower extent than DHP-dA-3

and DHP-dA-4 (Table 2). In contrast, rats dosed with either riddelliine or monocrotaline formed DHP-dG-3 and DHP-dG-4 as the major adducts, accompanied by small amounts of DHP-dA-3 and DHP-dA-4 (Tables 3 and 4).

On the basis of the results of our previous mechanistic studies conducted by ³²P-postlabeling/HPLC, we had proposed a general mechanism for DHP-derived DNA adduct formation from the metabolism of all three types of tumorigenic pyrrolizidine alkaloids (3, 5, 22, 24–26). Since the HPLC-ES-MS/MS method provides further insight regarding adduct formation, we have revised the proposed general metabolic activation mechanism, which is presented in Scheme 3. In this Scheme, the retronecine-, heliotridine-, and otonecine-type pyrrolizidine alkaloids are metabolized to reactive pyrrolic esters (3, 5, 22, 24–26). Hydrolysis and the subsequent loss of a hydroxyl group of the

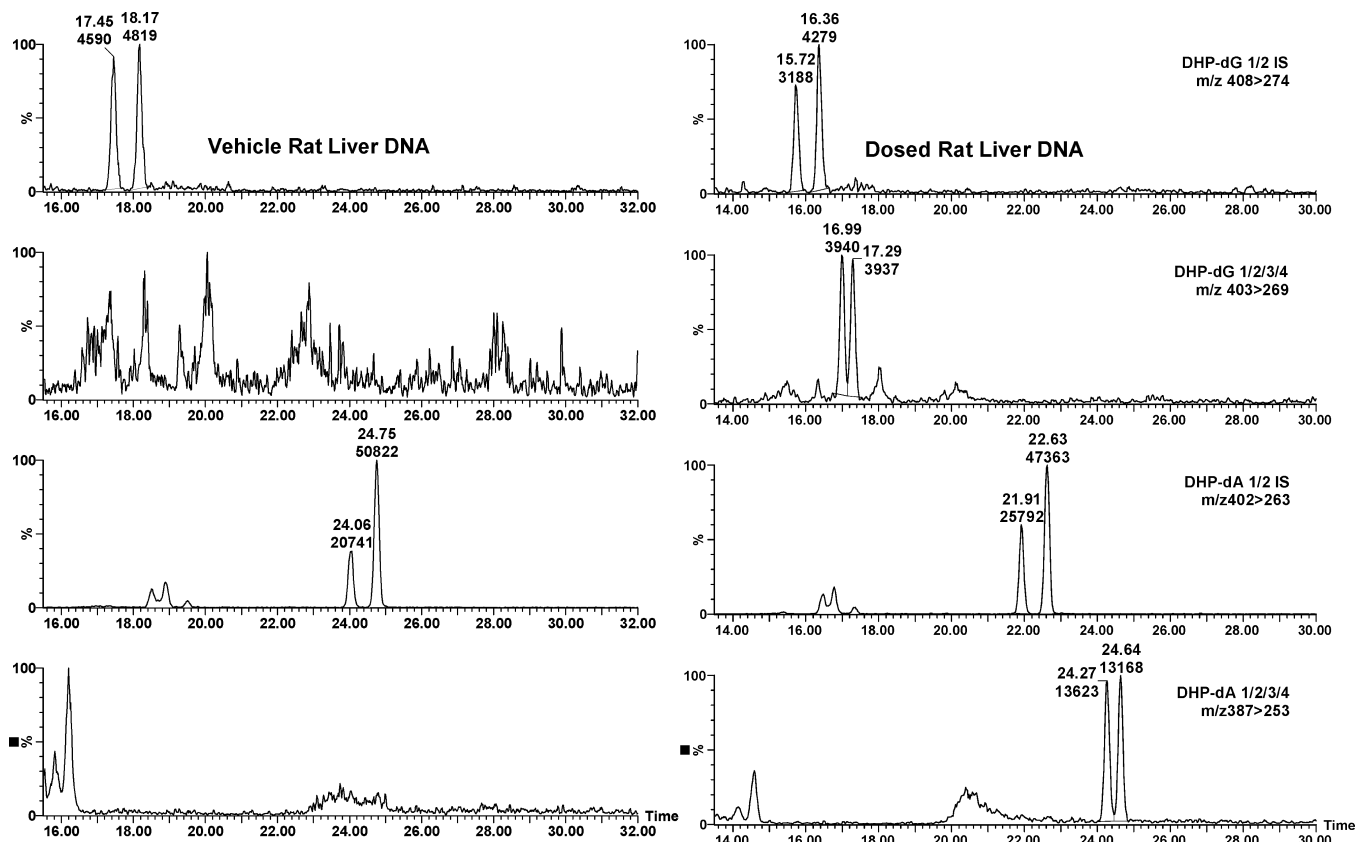


Figure 12. Representative MRM chromatograms (relative signal intensity vs time) for liver DNA samples from an NTP study in which female F344 rats were administered riddelliine. The left panel is a 100 μg aliquot of liver DNA from a control rat, and the right panel shows a 100 μg sample of DNA from a rat dosed at 1 mg of riddelliine/kg body weight five days/week for six months. Internal standards (IS) were added in amounts of 50, 55, 50, and 80 fmol for DHP-dG-1, DHP-dG-2, DHP-dA-1, and DHP-dA-2, respectively. The differences in retention times between the left and right panels are due to the use of two different HPLC columns.

Table 4. Levels of DHP-dG and DHP-dA Adducts Formed in the Livers of NTP Female Rats Dosed with Riddelliine for Six Months

riddelliine (mg/kg b.w./day)	levels of DHP-dG and DHP-dA/ 10^8 nucleotides ^a							
	DHP-dG-1	DHP-dG-2	DHP-dG-3	DHP-dG-4	DHP-dA-1	DHP-dA-2	DHP-dA-3	DHP-dA-4
1	<LOD	<LOD	5.9 ± 2.4	8.0 ± 2.4	<LOD	<LOD	0.5 ± 0.1	0.8 ± 0.2
0.33	<LOD	<LOD	2.3 ± 1.2	2.7 ± 1.2	<LOD	<LOD	0.3 ± 0.1	0.3 ± 0.1
0.1	<LOD	<LOD	<LOD	<LOD	<LOD	<LOD	0.1 ± 0.0	0.1 ± 0.1
0.1	<LOD	<LOD	<LOD	<LOD	<LOD	<LOD	<LOD	<LOD
0.033	<LOD	<LOD	<LOD	<LOD	<LOD	<LOD	<LOD	<LOD
0.01	<LOD	<LOD	<LOD	<LOD	<LOD	<LOD	<LOD	<LOD
0	<LOD	<LOD	<LOD	<LOD	<LOD	<LOD	<LOD	<LOD

^a Aliquots of DNA (100 μg) were assayed by HPLC-ES-MS/MS. The LOD for each of the adducts is given in Table 2. The data are presented as the mean \pm s.d., $n = 5$.

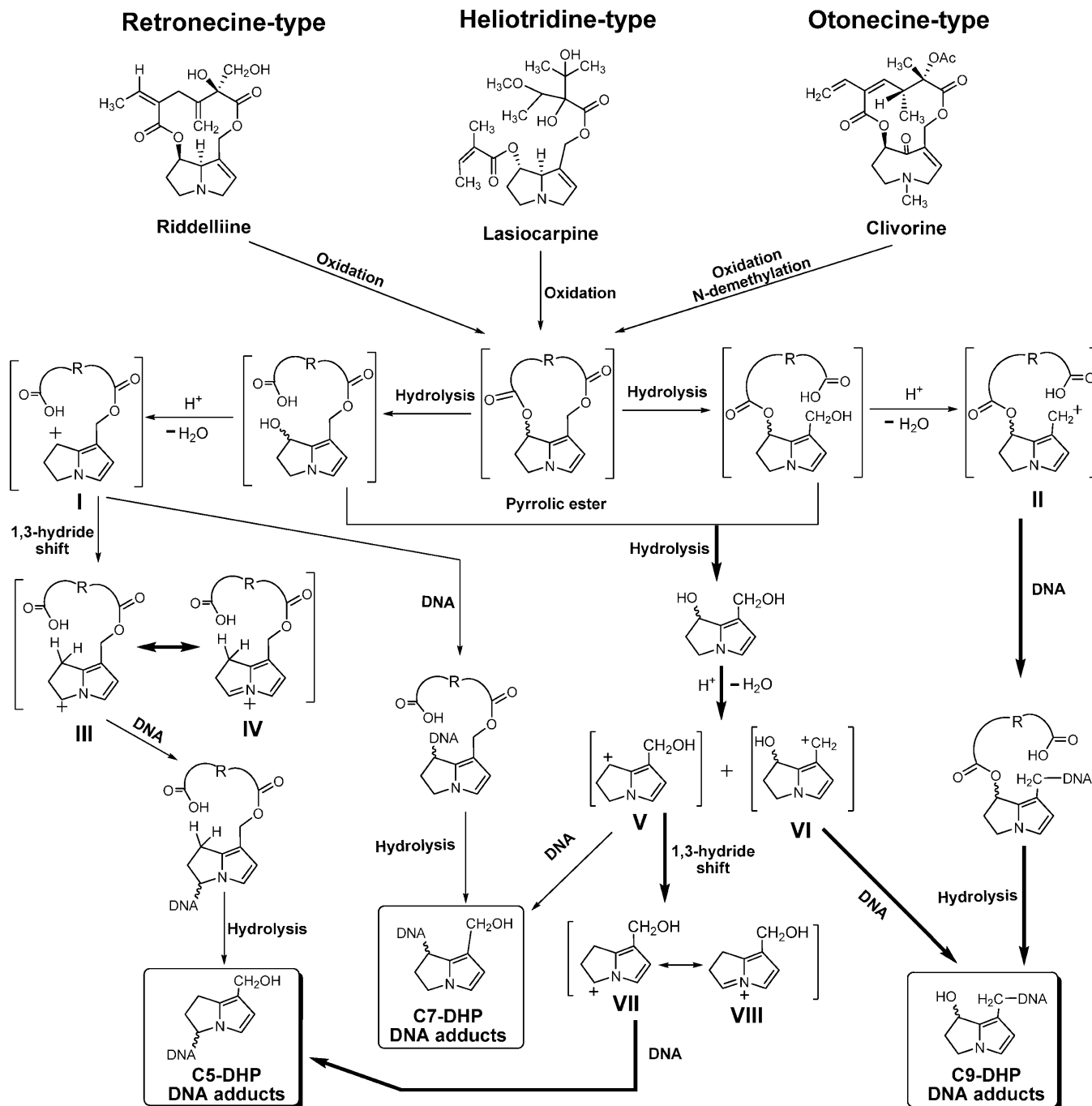
pyrrolic ester lead to the formation of carbonium ions I and II. Reaction of carbonium ion I with DNA produces C7-substituted DHP-DNA adducts (i.e., DHP-dG-1, DHP-dG-2, DHP-dA-1, and DHP-dA-2). Alternatively, carbonium ion I can undergo a 1,3-hydride shift to form carbonium ion III, which is stabilized through resonance with iminium ion IV. The reaction of carbonium ion III with DNA forms C5-substituted DHP-DNA adducts (i.e., DHP-dG-4), whereas the reaction of carbonium ion II with DNA leads to C9-substituted DHP-DNA adducts (i.e., DHP-dG-3).

The pyrrolic ester (shown in Scheme 3) can also undergo two consecutive hydrolysis steps to form DHP, which upon loss of a hydroxyl group forms carbonium ions V and VI. Reaction of these carbonium ions with DNA directly or after conversion into carbonium ion VII through a 1,3-hydride shift generates both DHP-C7 DNA adducts and DHP-C5 DNA adducts. The DHP-C7 DNA adducts formed from carbonium ion I should be kinetically controlled adducts, while the DHP-C5 DNA

adducts, mediated by the 1,3-hydride shift of carbonium ion I, should be thermodynamically controlled adducts.

A comparison of the ratio of adducts obtained from *in vitro* reactions with DHR indicates that steric hindrance plays a critical role in the regioselectivity of the reaction. When reactions are conducted between DHR and the nucleosides dG and dA, adducts arising from the reaction at C7 of DHP are formed to a greater extent than adducts arising from substitution at C5 or C9 of DHP. When DHR is reacted with DNA, the ratio between C7-substituted adducts remains the same, as is observed in the reactions with deoxynucleosides (DHP-dG-1/2:DHP-dA-1/2; $\sim 10:1$), while the proportion of adducts from reaction at C5 and/or C9 (i.e., DHP-dG-3/4 and DHP-dA-3/4) increases substantially (Table 2). This suggests that with the deoxynucleosides, reactions occur primarily with carbonium ion V, while with DNA, because of steric constraints, the equilibrium is shifted in favor of carbonium ions VI and VII (Scheme 3). The situation *in vivo* appears to be more complex. The only

Scheme 3. Proposed General Mechanism Leading to DHP-Derived DNA Adduct Formation from the Metabolism of the Three Types of Carcinogenic Pyrrolizidine Alkaloids^a



^a Riddelliine, lasiocarpine, and clivorine are used as examples for the retronecine-type, heliotridine-type, and otonecine-type pyrrolizidine alkaloids, respectively.

adducts detected in animals treated with riddelliine or monocrotaline are those obtained from the reaction at C5 and/or C9 of DHP (i.e., DHP-dG-3, DHP-dG-4, DHP-dA-3, and DHP-dA-4; Tables 3 and 4). The lack of adducts arising from substitution at C7 of DHP indicates that adduct formation *in vivo* does not occur with free DHR but rather must result from pathways involving carbonium ions I (which rearranges to carbonium ion III) and II, which leads to DHP-dG-3, DHP-dG-4, DHP-dA-3, and DHP-dA-4. The other possibility to explain the lack of DHP-dG-1, DHP-dG-2, DHP-dA-1, and DHP-dA-2 adduct formation *in vivo* is that these adducts are indeed formed but are readily repaired.

It is worthy to note that pyrrolizidine alkaloids are capable of binding at the C7 and the C9 positions of the necine base to two sites in DNA or protein to form DNA or protein cross-linking. The antimetabolic, toxic, and carcinogenic activities of pyrrolizidine alkaloids are thought to be caused, at least in part, by these cross-links (45–50). At present, it is not known whether or not DNA-interstrand cross-linking is involved, at least in part, in the observed DNA adduct formation profile *in vivo* and *in vitro*. It warrants further investigation.

On the basis of our comprehensive studies on the mechanisms of pyrrolizidine alkaloid carcinogenesis, we previously proposed that DHP-derived DNA adducts are potential

biomarkers of pyrrolizidine alkaloid exposure and tumorigenicity (3, 5, 8, 12, 20–22, 24–29, 51). With the new information obtained in the present study (Table 3, Table 4, and Scheme 3), the emphasis is focused on DHP-dG-3 and DHP-dG-4, and possibly DHP-dA-3 and DHP-dA-4. Riddelliine and monocrotaline, the two pyrrolizidine alkaloids studied by this HPLC-ES-MS/MS method, are retronecine-type pyrrolizidine alkaloids. The DNA adduct formation profiles from the metabolism of heliotridine-type and otonecine-type pyrrolizidine alkaloids have not yet been examined. In order to validate the generality of the proposed metabolic activation pathways shown in Scheme 3, mechanistic studies with these two types of pyrrolizidine alkaloids are needed.

Acknowledgment. We thank Dr. Po-Chuen Chan of NTP for supplying riddelliine and the NTP rat livers. This research was supported in part by appointments (Y.W. and Y.Z.) to the Postgraduate Research Program at the NCTR administered by the Oak Ridge Institute for Science and Education through an interagency agreement between the U.S. Department of Energy and the FDA. This article is not an official U.S. Food and Drug Administration (FDA) guidance or policy statement. No official support or endorsement by the U.S. FDA is intended or should be inferred.

References

- Roeder, E. (1995) Medicinal plants in Europe containing pyrrolizidine alkaloids. *Pharmazie* 50, 83–98.
- Roeder, E. (2000) Medicinal plants in China containing pyrrolizidine alkaloids. *Pharmazie* 55, 711–726.
- Fu, P. P., Xia, Q., Chou, M. W., and Lin, G. (2007) Detection, hepatotoxicity, and tumorigenicity of pyrrolizidine alkaloids in Chinese herbal plants and herbal dietary supplements. *J. Food Drug Anal.* 15, 400–415.
- Mattocks, A. R. (1986) *Chemistry and Toxicology of Pyrrolizidine Alkaloids*, Academic Press, London, UK.
- Fu, P. P., Xia, Q., Lin, G., and Chou, M. W. (2004) Pyrrolizidine alkaloids: genotoxicity, metabolism enzymes, metabolic activation, and mechanisms. *Drug Metab. Rev.* 36, 1–55.
- International Agency for Research in Cancer (IARC). (1976) Pyrrolizidine Alkaloids, in *IARC Monographs on the Evaluation of Carcinogenic Risk of Chemicals to Man: Some Naturally Occurring Substances*, International Agency for Research in Cancer, Lyon, France.
- Roeder, E., and Wiedenfeld, H. (2009) Pyrrolizidine alkaloids in medicinal plants of Mongolia, Nepal and Tibet. *Pharmazie* 64, 699–716.
- Fu, P. P., Yang, Y.-C., Xia, Q., Chou, M. W., Cui, Y. Y., and Lin, G. (2002) Pyrrolizidine alkaloids: tumorigenic components in Chinese herbal medicines and dietary supplements. *J. Food Drug Anal.* 10, 198–211.
- Bull, L. B., Culvenor, C. C. J., and Dick, A. J. (1968) *The Pyrrolizidine Alkaloids: Their Chemistry, Pathogenicity and Other Biological Properties*, North-Holland Publishing, Amsterdam, The Netherlands.
- International Programme on Chemical Safety (IPCS). (1989) *Pyrrolizidine Alkaloids Health and Safety Guide*, Health and Safety Criteria Guide 26, WHO, Geneva, Switzerland.
- Smith, L. W., and Culvenor, C. C. (1981) Plant sources of hepatotoxic pyrrolizidine alkaloids. *J. Nat. Prod.* 44, 129–152.
- Fu, P., Chou, M., Xia, Q., Yang, Y.-C., Yan, J., Doerge, D., and Chan, P. (2001) Genotoxic pyrrolizidine alkaloids and pyrrolizidine alkaloid N-oxides: mechanisms leading to DNA adduct formation and tumorigenicity. *J. Environ. Sci. Health, Part C* 19, 353–386.
- Stegemeier, B. L., Edgar, J. A., Colegate, S. M., Gardner, D. R., Schoch, T. K., Coulombe, R. A., and Molyneux, R. J. (1999) Pyrrolizidine alkaloid plants, metabolism and toxicity. *J. Nat. Toxins* 8, 95–116.
- Huxtable, R. J. (1980) Herbal teas and toxins: novel aspects of pyrrolizidine poisoning in the United States. *Perspect. Biol. Med.* 24, 1–14.
- Steenkamp, V., Stewart, M. J., and Zuckerman, M. (2000) Clinical and analytical aspects of pyrrolizidine poisoning caused by South African traditional medicines. *Ther. Drug Monit.* 22, 302–306.
- Schoental, R., Head, M. A., and Peacock, P. R. (1954) Senecio alkaloids; primary liver tumours in rats as a result of treatment with (1) a mixture of alkaloids from *S. jacobaea* Lin.; (2) retrorsine; (3) isatidine. *Br. J. Cancer* 8, 458–465.
- National Toxicology Program. (1978) *TR-39 Bioassay of Lasiocarpine for Possible Carcinogenicity (CAS No. 303-34-4)*, NIH Publication No. 78-839, U.S. Department of Health and Human Services, Public Health Service, National Institutes of Health, Research Triangle Park, NC.
- National Toxicology Program. (2003) *TR-508 Toxicology and Carcinogenesis Studies of Riddelliine (CAS No. 23246-96-0) in F344/N Rats and B6C3F1 Mice (Gavage Studies)*, NIH Publication No. 03-4442, U.S. Department of Health and Human Services, Public Health Service, National Institutes of Health, Research Triangle Park, NC.
- Yang, Y. C., Yan, J., Doerge, D. R., Chan, P. C., Fu, P. P., and Chou, M. W. (2001) Metabolic activation of the tumorigenic pyrrolizidine alkaloid, riddelliine, leading to DNA adduct formation in vivo. *Chem. Res. Toxicol.* 14, 101–109.
- Chou, M. W., Yan, J., Nichols, J., Xia, Q., Beland, F. A., Chan, P.-C., and Fu, P. P. (2003) Correlation of DNA adduct formation and riddelliine-induced liver tumorigenesis in F344 rats and B6C3F1 mice. *Cancer Lett.* 193, 119–125.
- Chou, M. W., Jian, Y., Williams, L. D., Xia, Q., Churchwell, M., Doerge, D. R., and Fu, P. P. (2003) Identification of DNA adducts derived from riddelliine, a carcinogenic pyrrolizidine alkaloid, in vitro and in vivo. *Chem. Res. Toxicol.* 16, 1130–1137.
- Xia, Q., Chou, M. W., Kadlubar, F. F., Chan, P.-C., and Fu, P. P. (2003) Human liver microsomal metabolism and DNA adduct formation of the tumorigenic pyrrolizidine alkaloid, riddelliine. *Chem. Res. Toxicol.* 16, 66–73.
- Federal Register. (2008) 73, 23463.
- Xia, Q., Chou, M. W., Lin, G., and Fu, P. P. (2004) Metabolic formation of DHP-derived DNA adducts from a representative otonecine type pyrrolizidine alkaloid clivorine and the extract of *Ligularia hodgsonii* hook. *Chem. Res. Toxicol.* 17, 702–708.
- Xia, Q., Chou, M. W., Edgar, J. A., Doerge, D. R., and Fu, P. P. (2006) Formation of DHP-derived DNA adducts from metabolic activation of the prototype heliotridine-type pyrrolizidine alkaloid, lasiocarpine. *Cancer Lett.* 231, 138–145.
- Xia, Q., Yan, J., Chou, M. W., and Fu, P. P. (2008) Formation of DHP-derived DNA adducts from metabolic activation of the prototype heliotridine-type pyrrolizidine alkaloid, heliotrine. *Toxicol. Lett.* 178, 77–82.
- Wang, Y.-P., Fu, P., and Chou, M. (2005) Metabolic activation of the tumorigenic pyrrolizidine alkaloid, retrorsine, leading to DNA adduct formation in vivo. *Int. J. Environ. Res. Pub. Health* 2, 74–79.
- Wang, Y.-P., Yan, J., Beger, R. D., Fu, P. P., and Chou, M. W. (2005) Metabolic activation of the tumorigenic pyrrolizidine alkaloid, monocrotaline, leading to DNA adduct formation in vivo. *Cancer Lett.* 226, 27–35.
- Yan, J., Xia, Q., Chou, M. W., and Fu, P. P. (2008) Metabolic activation of retronecine and retronecine N-oxide: formation of DHP-derived DNA adducts. *Toxicol. Ind. Health* 24, 181–188.
- Yan, J., Nichols, J., Yang, Y.-C., Fu, P., and Chou, M. (2002) Detection of riddelliine-derived DNA adducts in blood of rats fed riddelliine. *Int. J. Mol. Sci.* 3, 1019–1026.
- Mattocks, A. R. (1968) Toxicity of pyrrolizidine alkaloids. *Nature* 217, 723–728.
- Chauvin, P., Dillon, J. C., and Moren, A. (1994) An outbreak of Heliotrope food poisoning, Tadjikistan, November 1992-March 1993, *Sante* 4, 263–268.
- Prakash, A. S., Pereira, T. N., Reilly, P. E., and Seawright, A. A. (1999) Pyrrolizidine alkaloids in human diet. *Mutat. Res.* 443, 53–67.
- Byron, J. (1998) Pyrrolizidine alkaloids in eggs; new alkaloid found in potatoes. *Food Chem. News* 14, 6–7.
- Culvenor, C. C. J., Edgar, J. A., Smith, J. A., and Hirono, I. (1976) The occurrence of senecionine in *Tussilago farfara*. *Aust. J. Chem.* 29, 229–230.
- Winship, K. A. (1991) Toxicity of comfrey. *Adverse Drug React. Toxicol. Rev.* 10, 47–59.
- Huxtable, R. J. (1989) Human Health Implications of Pyrrolizidine Alkaloids and the Herbs Containing them, in *Toxicants of Plant Origin*, Vol. 1 Alkaloids, pp 41–86 (Cheeke, P. R., Ed.) CRC Press, Boca Raton, FL.
- Edgar, J. A., Roeder, E., and Molyneux, R. J. (2002) Honey from plants containing pyrrolizidine alkaloids: a potential threat to health. *J. Agric. Food Chem.* 50, 2719–2730.
- Betz, J. M., Eppley, R. M., Taylor, W. C., and Andrzejewski, D. (1994) Determination of pyrrolizidine alkaloids in commercial comfrey products (*Symphytum* sp.). *J. Pharm. Sci.* 83, 649–653.
- Chou, M. W., and Fu, P. P. (2006) Formation of DHP-derived DNA adducts in vivo from dietary supplements and Chinese herbal plant extracts containing carcinogenic pyrrolizidine alkaloids. *Toxicol. Ind. Health* 22, 321–327.

- (41) Yang, Y.-C., Yan, J., Churchwell, M., Beger, R., Chan, P.-C., Doerge, D. R., Fu, P. P., and Chou, M. W. (2001) Development of a ^{32}P -postlabeling/HPLC method for detection of dehydroretrotronecine-derived DNA adducts in vivo and in vitro. *Chem. Res. Toxicol.* *14*, 91–100.
- (42) Chan, P. C., Haseman, J. K., Prejean, J. D., and Nyska, A. (2003) Toxicity and carcinogenicity of riddelliine in rats and mice. *Toxicol. Lett.* *144*, 295–311.
- (43) Beland, F. A., Churchwell, M. I., Von Tungeln, L. S., Chen, S., Fu, P. P., Culp, S. J., Schoket, B., Gyorffy, E., Minarovits, J., Poirier, M. C., Bowman, E. D., Weston, A., and Doerge, D. R. (2005) High-performance liquid chromatography electrospray ionization tandem mass spectrometry for the detection and quantitation of benzo[a]pyrene-DNA adducts. *Chem. Res. Toxicol.* *18*, 1306–1315.
- (44) Robertson, K. A. (1982) Alkylation of N^2 in deoxyguanosine by dehydroretrotronecine, a carcinogenic metabolite of the pyrrolizidine alkaloid monocrotaline. *Cancer Res.* *42*, 8–14.
- (45) Hincks, J. R., Kim, H. Y., Segall, H. J., Molyneux, R. J., Stermitz, F. R., and Coulombe, R. A. (1991) DNA cross-linking in mammalian cells by pyrrolizidine alkaloids: structure-activity relationships. *Toxicol. Appl. Pharmacol.* *111*, 90–98.
- (46) Kim, H. Y., Stermitz, F. R., Molyneux, R. J., Wilson, D. W., Taylor, D., and Coulombe, R. A. (1993) Structural influences on pyrrolizidine alkaloid-induced cytopathology. *Toxicol. Appl. Pharmacol.* *122*, 61–69.
- (47) Kim, H. Y., Stermitz, F. R., and Coulombe, R. A. (1995) Pyrrolizidine alkaloid-induced DNA-protein cross-links. *Carcinogenesis* *16*, 2691–2697.
- (48) Coulombe, R. A., Jr., Drew, G. L., and Stermitz, F. R. (1999) Pyrrolizidine alkaloids crosslink DNA with actin. *Toxicol. Appl. Pharmacol.* *154*, 198–202.
- (49) Kim, H. Y., Stermitz, F. R., Li, J. K., and Coulombe, R. A., Jr. (1999) Comparative DNA cross-linking by activated pyrrolizidine alkaloids. *Food Chem. Toxicol.* *37*, 619–625.
- (50) Rieben, W. K., Jr., and Coulombe, R. A., Jr. (2004) DNA Cross-linking by dehydromonocrotaline lacks apparent base sequence preference. *Toxicol. Sci.* *82*, 1–25.
- (51) Fu, P., Xia, Q., Lin, G., and Chou, M. (2002) Genotoxic pyrrolizidine alkaloids: mechanisms leading to DNA adduct formation and tumorigenicity. *Int. J. Mol. Sci.* *3*, 948–964.

TX900402X